

# Full Boltzmann equations for leptogenesis including scattering

---

**F. Hahn-Woernle<sup>1</sup>, M. Plümacher<sup>1</sup> and Y. Y. Y. Wong<sup>2,3</sup>**

<sup>1</sup>*Max-Planck-Institut für Physik, Föhringer Ring 6, D-80805 München, Germany*

<sup>2</sup>*Theory Division, Physics Department, CERN, CH-1211 Geneva 23, Switzerland*

<sup>3</sup>*Institut für Theoretische Physik E, RWTH Aachen University, D-52056 Aachen, Germany*

**ABSTRACT:** We study the evolution of a cosmological baryon asymmetry produced via leptogenesis by means of the full classical Boltzmann equations, without the assumption of kinetic equilibrium and including all quantum statistical factors. Beginning with the full mode equations, we derive the usual equations of motion for the right-handed neutrino number density and integrated lepton asymmetry, and show explicitly the impact of each assumption on these quantities. For the first time, we investigate also the effects of scattering of the right-handed neutrino with the top quark to leading order in the Yukawa couplings by means of the full Boltzmann equations. We find that in our full Boltzmann treatment the final lepton asymmetry can be suppressed by as much as a factor of  $\sim 1.5$  in the weak wash-out regime ( $K \lesssim 1$ ), compared to the usual integrated approach which assumes kinetic equilibrium and neglects quantum statistics. This suppression is in contrast with the enhancement seen in some previous studies that considered only decay and inverse decay of the right-handed neutrino. However, this suppression quickly decreases as we increase  $K$ . In the strong wash-out regime ( $K \gtrsim 1$ ), the full Boltzmann treatment and the integrated approach give nearly identical final lepton asymmetries (within 10% of each other at  $K > 3$ ). Finally, we show that the opposing effects of quantum statistics on decays/inverse decays and the scattering processes tend to reduce the net importance of scattering on leptogenesis in the full treatment compared to the integrated approach.

---

## Contents

<b>1. Introduction</b>	<b>1</b>
<b>2. Basic set-up</b>	<b>2</b>
<b>3. Decay and inverse decay</b>	<b>4</b>
3.1 Case D1: Integrated Boltzmann equations	5
3.2 Case D2: Dropping the assumption of kinetic equilibrium	8
3.3 Case D3: Boltzmann equations with quantum statistical factors	9
3.4 Case D4: Complete mode equations	10
3.5 Results and discussions	10
3.5.1 Right-handed neutrino	10
3.5.2 Lepton asymmetry	12
<b>4. Scattering processes</b>	<b>13</b>
4.1 Case S1: Scattering in the integrated picture	14
4.2 Case S2: Complete mode equations including scattering	17
4.3 Results and discussions	17
4.3.1 Scattering vs decay–inverse decay	17
4.3.2 Complete treatment vs integrated approach	20
<b>5. Conclusions</b>	<b>22</b>
<b>A. Reduction of the scattering collision integrals</b>	<b>24</b>
A.1 $s$ -channel	24
A.1.1 Right-handed neutrino	24
A.1.2 Lepton asymmetry	30
A.2 $t$ -channel	31
A.2.1 Right-handed neutrino	31
A.2.2 Lepton asymmetry	34
<b>B. Evolution of the top Yukawa coupling</b>	<b>35</b>

---

## 1. Introduction

Leptogenesis [1] provides an attractive explanation for the baryon asymmetry of the universe. The ingredients of this mechanism are simple: heavy right-handed Majorana neutrinos are added to the standard model of particle physics, which on the one hand explains naturally the smallness of the

observed neutrino masses by way of the see-saw mechanism [2]. On the other hand, the out-of-equilibrium decay of the heavy neutrino states into leptons and Higgs particles violates  $CP$ , from whence a lepton asymmetry can be generated. This lepton asymmetry is then partially transformed into a baryon asymmetry by anomalous processes of the standard model called sphalerons [3].

In the recent past a huge step forward has been made towards understanding in detail the processes of leptogenesis. Relevant studies include leptogenesis in a supersymmetric context [4], thermal effects [5, 6], analytic formulae for the final efficiency factor [7], the role of flavour [8, 9, 10, 11], as well as leptogenesis with  $CP$  violation coming only from the measurable low-scale Pontecorvo–Maki–Nakagawa–Sakata matrix [12]. Furthermore, it has been pointed out that the classical Boltzmann equations are insufficient to describe the transition region between the flavoured and the unflavoured regimes [13]; a full quantum-mechanical description in terms of density matrices is necessary. On this front, the quantum-mechanical Kadanoff–Baym equations have been investigated for toy models in extreme out-of-equilibrium situations [14, 15].

On a different front, the classical Boltzmann equations have been solved for the first time for single momentum modes [16]. As one of Sakharov’s conditions [17], departure from thermal equilibrium is crucial for the dynamic creation of a baryon asymmetry. In the leptogenesis scenario, out-of-equilibrium conditions are achieved when interactions are no longer able to maintain the momentum distribution function of the right-handed neutrino at its equilibrium value as the universe expands. To simplify the calculation, this non-equilibrium process is traditionally studied by means of the integrated Boltzmann equations [6, 18, 19, 20], whereby the equations of motion for the distribution functions of all particle species involved are integrated over momentum such that only the evolution of the *number densities* is tracked. However, in order for the integrated equations to be in a closed form, it is necessary to neglect quantum statistical behaviours (e.g., Pauli blocking) and assume kinetic equilibrium for all particle species, including the right-handed neutrino. For particle species with gauge interactions these assumptions seem justifiable. For the right-handed neutrino however, their validity is not immediately obvious.

To estimate the effects of kinetic equilibrium and quantum statistics, the Boltzmann equations for the individual momentum modes have been solved in [16], taking into account only the decay and inverse decay of the right-handed neutrino within the unflavoured framework. More recently, the mode equations have been used to study the effect of a pre-existing asymmetry and the soft leptogenesis scenario, again including only decays and inverse decays [21]. In the present work, we extend on these previous studies by considering also scattering processes of the right-handed neutrino with the top quark.

The paper is organised as follows: We describe the basic set-up of our scenario in section 2. In section 3 we study the simplest scenario involving only the decay and inverse decay of the right-handed neutrino. In section 4 we include scattering processes mediated by the Yukawa interaction of heavy neutrinos with the top quark. We conclude in section 5.

## 2. Basic set-up

We concentrate on the simplest case of “vanilla-leptogenesis”, in which a lepton asymmetry is established from the decay and scattering of the lightest heavy right-handed neutrino  $N_1$ . We neglect the decay of the two heavier neutrino states  $N_{2,3}$  [22], assuming that any lepton asymmetry pro-

duced from these decays will be efficiently washed out by the  $N_1$  interactions. Therefore we will drop the subscript “1”, and refer to the lightest right-handed neutrino simply as  $N$  in the following. Furthermore we will work in the one-flavour approximation, since flavour effects do not change the kinetic consideration for the mode equations.

Generally, the Boltzmann equation (BE) for a right-handed neutrino (RHN) in a Friedman–Lemaître–Robertson–Walker framework can be written as

$$\frac{\partial f_N}{\partial t} - |\mathbf{p}_N| H \frac{\partial f_N}{\partial |\mathbf{p}_N|} = C_D [f_N] + C_S [f_N], \quad (2.1)$$

where  $f_N$  is the phase space distribution of the RHN,  $\mathbf{p}_N$  the RHN momentum, and  $H$  the Hubble parameter. On the right-hand side, the collision integrals  $C_D [f_N]$  and  $C_S [f_N]$  encode respectively the interactions of the RHN due to decays into leptons and Higgs ( $D$ ) and scattering processes via Yukawa interactions with the top quark ( $S$ ).

The Boltzmann equation for leptons (anti-leptons) with phase space distribution  $f_l$  ( $f_{\bar{l}}$ ) has a similar form to Eq. (2.1), save for the replacements  $f_N \rightarrow f_l$  ( $f_N \rightarrow f_{\bar{l}}$ ) and  $\mathbf{p}_N \rightarrow \mathbf{p}_l$  ( $\mathbf{p}_N \rightarrow \mathbf{p}_{\bar{l}}$ ). Since we are interested in the asymmetry between leptons and antileptons, it is convenient to define

$$f_{l-\bar{l}} \equiv f_l - f_{\bar{l}}, \quad (2.2)$$

and the corresponding Boltzmann equation

$$\frac{\partial f_{l-\bar{l}}}{\partial t} - |\mathbf{p}_l| H \frac{\partial f_{l-\bar{l}}}{\partial |\mathbf{p}_l|} = C_D [f_{l-\bar{l}}] + C_S [f_{l-\bar{l}}], \quad (2.3)$$

where  $C_{D,S} [f_{l-\bar{l}}] \equiv C_{D,S} [f_l] - C_{D,S} [f_{\bar{l}}]$ . Integrating  $f_{l-\bar{l}}$  over the lepton phase space, i.e.,

$$n_{l-\bar{l}} \equiv \frac{g_l}{(2\pi)^3} \int d^3 p_l f_{l-\bar{l}}, \quad (2.4)$$

with  $g_l = 2$ , gives us the lepton asymmetry per co-moving photon,

$$N_{l-\bar{l}} \equiv \frac{n_{l-\bar{l}}}{n_\gamma^{\text{eq}}}, \quad (2.5)$$

where  $n_\gamma^{\text{eq}} = (\zeta(3)/\pi^2) g_\gamma T^3$ , with  $g_\gamma = 2$ , is the equilibrium photon density.

Equations (2.1) and (2.3) can be further simplified by transforming to the dimensionless coordinates  $z = M/T$  and  $y_i = |\mathbf{p}_i|/T$ , where  $M$  is the mass of the RHN [23]. Using the relation  $dT/dt = -HT$ , the differential operator  $\partial_t - |\mathbf{p}_i| H \partial_{|\mathbf{p}_i|}$  becomes  $zH\partial_z$ , and consequently

$$\frac{\partial f_N(z, y)}{\partial z} = \frac{z}{H(M)} (C_D [f_N(z, y)] + C_S [f_N(z, y)]), \quad (2.6)$$

and

$$\frac{\partial f_{l-\bar{l}}(z, y)}{\partial z} = \frac{z}{H(M)} (C_D [f_{l-\bar{l}}(z, y)] + C_S [f_{l-\bar{l}}(z, y)]), \quad (2.7)$$

with  $H(M) = \sqrt{4\pi^3 g^*/45} (M/M_{\text{Pl}})$ , where  $M_{\text{Pl}} = 1.221 \times 10^{19}$  GeV is the Planck mass, and  $g^* = 106.75$  corresponds to the number of relativistic degrees of freedom in the standard model at temperatures higher than the electroweak scale.

The Boltzmann equations (2.6) and (2.7) encode how a lepton asymmetry is generated and washed out in an expanding universe given some specific particle interactions. Here, it is useful to define an efficiency factor that measures the amount of asymmetry that has survived the competitive production and wash-out processes,

$$\kappa \equiv \frac{4}{3} \varepsilon^{-1} N_{l-\bar{l}}. \quad (2.8)$$

The quantity  $\varepsilon$  quantifies the amount of  $CP$  violation in the interactions, while  $N_{l-\bar{l}}$  is the lepton asymmetry produced. In the limit of a vanishing wash-out and a thermal initial abundance for the RHN, the efficiency factor has a final value  $\kappa_f = 1$ .

### 3. Decay and inverse decay

We consider first the simplest possible scenario of thermal leptogenesis, in which only the decay and inverse decay of the RHN into lepton  $l$  and Higgs  $\Phi$  pairs contribute to the evolution of  $f_N$ , i.e., we set  $C_S = 0$  in Eqs. (2.6) and (2.7). The decay and inverse decay of the RHN violate  $CP$  through interference of the tree-level and the one-loop diagrams.

The collision integral for the RHN in the decay–inverse decay picture has the following form:

$$\begin{aligned} C_D[f_N] = & \frac{1}{2E_N} \int \frac{d^3p_l}{2E_l(2\pi)^3} \frac{d^3p_\Phi}{2E_\Phi(2\pi)^3} (2\pi)^4 \delta^4(p_N - p_l - p_\Phi) \\ & \times [f_\Phi f_l (1 - f_N) (|\mathcal{M}_{\Phi l \rightarrow N}|^2 + |\mathcal{M}_{\Phi \bar{l} \rightarrow N}|^2) \\ & - f_N (1 - f_l) (1 + f_\Phi) (|\mathcal{M}_{N \rightarrow \Phi l}|^2 + |\mathcal{M}_{N \rightarrow \Phi \bar{l}}|^2)], \end{aligned} \quad (3.1)$$

where  $E_i$  and  $p_i$  are, respectively, the energy and 4-momenta of the particle species  $i$ , and  $\mathcal{M}_A$  denotes the matrix element for the process  $A$ . At tree level, the squared matrix element summed over all internal degrees of freedom for the decay of the RHN into a pair of lepton and Higgs particles is given by

$$|\mathcal{M}_{N \rightarrow \Phi l}|^2 = 2 \frac{(m_D^\dagger m_D)_{11}}{v^2} p_l p_N, \quad (3.2)$$

where  $v = 174 \text{ GeV}$  is the vacuum expectation value of the Higgs particle, and the Dirac mass matrix  $m_D$  is connected to the Yukawa coupling matrix  $\lambda_\nu$  via  $m_D = v\lambda_\nu$ .

The integral (3.1) can be readily reduced to a one dimensional form [24]

$$C_D[f_N] = \frac{M\Gamma_{\text{rf}}}{E_N p_N} \int_{(E_N - p_N)/2}^{(E_N + p_N)/2} dp_\Phi [f_\Phi f_l (1 - f_N) - f_N (1 - f_l) (1 + f_\Phi)], \quad (3.3)$$

where

$$\Gamma_{\text{rf}} = \frac{\tilde{m}_1 M^2}{8\pi v^2} \quad (3.4)$$

is the total decay rate in the RHN's rest frame, with

$$\tilde{m}_1 = \frac{(m_D^\dagger m_D)_{11}}{M} \quad (3.5)$$

the *effective neutrino mass* [20], to be compared with the *equilibrium neutrino mass*

$$m_* = \frac{16\pi^{\frac{5}{2}} \sqrt{g^*} v^2}{3\sqrt{5} M_{Pl}}. \quad (3.6)$$

The decay parameter

$$K \equiv \frac{\Gamma_{\text{rf}}}{H(M)} = \frac{\tilde{m}_1}{m_*} \quad (3.7)$$

controls whether the RHN decays in equilibrium ( $K > 1$ ) or out of equilibrium ( $K < 1$ ).

For leptons participating in the same decay and inverse decay processes, the collisional integral is given by

$$\begin{aligned} C_D[f_l] = & \frac{1}{2E_l} \int \frac{d^3p_N}{2E_N(2\pi)^3} \frac{d^3p_\Phi}{2E_\Phi(2\pi)^3} (2\pi)^4 \delta^4(p_N - p_l - p_\Phi) \\ & \times [f_N(1-f_l)(1+f_\Phi)|\mathcal{M}_{N \rightarrow \Phi l}|^2 \\ & - f_\Phi f_l(1-f_N)|\mathcal{M}_{\Phi l \rightarrow N}|^2]. \end{aligned} \quad (3.8)$$

An analogous expression for the anti-leptons can be derived by replacing  $f_l \rightarrow f_{\bar{l}}$ ,  $\mathcal{M}_{N \rightarrow \Phi l} \rightarrow \mathcal{M}_{N \rightarrow \Phi \bar{l}}$ , and  $\mathcal{M}_{\Phi l \rightarrow N} \rightarrow \mathcal{M}_{\Phi \bar{l} \rightarrow N}$ . Some useful relations exist between the matrix elements following from  $CPT$ -invariance [18]:

$$\begin{aligned} |\mathcal{M}_{N \rightarrow \Phi l}|^2 &= |\mathcal{M}_{\Phi \bar{l} \rightarrow N}|^2 = |\mathcal{M}_0|^2(1+\varepsilon), \\ |\mathcal{M}_{N \rightarrow \Phi \bar{l}}|^2 &= |\mathcal{M}_{\Phi l \rightarrow N}|^2 = |\mathcal{M}_0|^2(1-\varepsilon), \end{aligned} \quad (3.9)$$

where  $|\mathcal{M}_0|^2$  is the tree level matrix element given in Eq. (3.2).

The collision integral (3.8) suffers from the problem that a lepton asymmetry is produced even in thermal equilibrium. This can be remedied by including contributions from the resonant part of the  $\Delta L = 2$  scattering process  $l\Phi \leftrightarrow \bar{l}\Phi$  [6, 18]. We implement this remedy following the method developed in [7], and add to the collision integral (3.8) the term

$$f_\Phi f_{\bar{l}}(1-f_N)|\mathcal{M}_{\Phi \bar{l} \rightarrow N}|_{\text{sub}}^2 - f_\Phi f_l(1-f_N)|\mathcal{M}_{\Phi l \rightarrow N}|_{\text{sub}}^2, \quad (3.10)$$

where

$$\begin{aligned} |\mathcal{M}_{\Phi \bar{l} \rightarrow N}|_{\text{sub}}^2 &= |\mathcal{M}_{\Delta L=2}^2 - \varepsilon|\mathcal{M}_0|^2, \\ |\mathcal{M}_{\Phi l \rightarrow N}|_{\text{sub}}^2 &= |\mathcal{M}_{\Delta L=2}^2 + \varepsilon|\mathcal{M}_0|^2, \end{aligned} \quad (3.11)$$

where  $|\mathcal{M}_{\Delta L=2}^2$  is negligible for  $M \ll 10^{14}$  GeV [25].<sup>1</sup>

In the following subsections, we review first the derivation of the conventional integrated Boltzmann equations, which neglects quantum statistics and assumes kinetic equilibrium for the RHN. We then remove step by step these assumptions, in order to examine their effects on the efficiency factor  $\kappa$ . The scenarios to be examined and their associated assumptions are summarised in table 1.

### 3.1 Case D1: Integrated Boltzmann equations

In the integrated approach conventionally used in the literature [6, 7, 18], the time evolution of number densities  $n_i$  are tracked in favour of the phase space distributions  $f_i$ . This is achieved by integrating the Boltzmann equations (2.6) and (2.7) over momentum. However, the integrated equations have no closed forms unless we make certain simplifying assumptions: First, we neglect factors stemming from Pauli blocking for fermions and induced emission for bosons, i.e.,

<sup>1</sup>Reference [21] includes terms in addition to Eq. (3.10) in order to avoid asymmetry production in thermal equilibrium. However, the same analysis also shows that the quantitative difference between this and our approach is negligible.

**Table 1:** Scenarios considered in the decay/inverse decay picture and their associated assumptions. Case D1 corresponds to the conventional integrated Boltzmann approach, while Case D4 was previously investigated by Basbøll and Hannestad [16].

	Assumption of kinetic equilibrium	Including quantum statistics	Section
Case D1	Yes	No	3.1
Case D2	No	No	3.2
Case D3	Yes	Yes	3.3
Case D4	No	Yes	3.4

we approximate  $1 \pm f_i \approx 1$  [18]. Second, all standard model particles are taken to be in thermal equilibrium due to their gauge interactions and their distribution functions approximated by a Maxwell–Boltzmann distribution,  $f_i^{\text{eq}} = e^{-E_i/T}$ .

With these assumptions and using energy conservation, we find

$$f_\Phi f_l = e^{-(E_\Phi + E_l)/T} = e^{-E_N/T} = f_N^{\text{eq}}, \quad (3.12)$$

so that the collision integral (3.3) simplifies to

$$C_D[f_N] = \frac{M\Gamma_{\text{rf}}}{E_N p_N} \int_{(E_N - p_N)/2}^{(E_N + p_N)/2} dp_\Phi [f_N^{\text{eq}} - f_N]. \quad (3.13)$$

Integrating (3.13) over  $p_\Phi$  and inserting into Eq. (2.6), the BE for the RHN distribution function becomes

$$\frac{\partial f_N}{\partial z} = \frac{z \Gamma_{\text{rf}} M}{H(M) E_N} (f_N^{\text{eq}} - f_N). \quad (3.14)$$

To make further inroads, we assume kinetic equilibrium holds for the RHN, i.e., its distribution function  $f_N$  can be expressed as  $f_N/f_N^{\text{eq}} \approx n_N/n_N^{\text{eq}}$ , where  $n_N$  is the RHN number density. Then one can easily integrate Eq. (3.14) over the RHN phase space to obtain

$$\frac{\partial n_N}{\partial z} = z K \left\langle \frac{M}{E_N} \right\rangle (n_N^{\text{eq}} - n_N), \quad (3.15)$$

where  $K \equiv \Gamma_{\text{rf}}/H(M)$  (cf. Eq. (3.7)), and  $\Gamma_{\text{rf}} \langle M/E_N \rangle \equiv (\Gamma_{\text{rf}}/n_N^{\text{eq}}) \int d^3 p_N / (2\pi)^3 f_N^{\text{eq}} (M/E_N)$  is the thermal average of the decay rate [18]. The thermally averaged dilation factor is given by the ratio of the modified Bessel functions of the second kind of first and second order,  $\langle M/E_N \rangle = K_1(z)/K_2(z)$ .

Dividing Eq. (3.15) by the equilibrium photon density  $n_\gamma^{\text{eq}}$ , we obtain the Boltzmann equation for the quantity  $N_N \equiv n_N/n_\gamma^{\text{eq}}$  [7],

$$\frac{\partial N_N}{\partial z} = -D (N_N - N_N^{\text{eq}}), \quad (3.16)$$

with

$$D \equiv z K \left\langle \frac{M}{E_N} \right\rangle, \quad (3.17)$$

and

$$N_N^{\text{eq}}(z) = \frac{3}{8} z^2 K_2(z). \quad (3.18)$$

Here, an inconsistency in the integrated approach is visible: all particles, i.e.,  $N$ ,  $l$  and  $\Phi$ , are assumed to follow the Maxwell–Boltzmann distribution function. However, when calculating  $N_N^{\text{eq}}$ , we must use a Fermi–Dirac distribution for the RHN,  $n_N^{\text{eq}} = [3\zeta(3)g_N T M^2/(8\pi^2)] K_2(z)$ , with  $\zeta(3) \approx 1.202$  and  $g_N = 2$ , in order to reproduce a realistic equilibrium RHN to photon density ratio. This leads to an extra prefactor  $(3/4)\zeta(3)$  in the definition of  $N_N^{\text{eq}}$  compared to a strictly Maxwell–Boltzmann approach.

For the lepton asymmetry, Eqs. (2.7), (3.8) and (3.10) combine to give the BE for the lepton distribution functions,

$$\frac{\partial f_{l-\bar{l}}}{\partial z} = -\frac{z^2 K}{2y_l^2} \int_{\frac{z^2-4y_l^2}{4y_l}}^{\infty} dy_N \frac{y_N}{\mathcal{E}_N} [f_\Phi f_{l-\bar{l}} - 2\varepsilon (f_N - f_N^{\text{eq}})], \quad (3.19)$$

where  $\mathcal{E}_N \equiv E_N/T$ . Using energy conservation and assuming kinetic equilibrium for the RHN, Eq. (3.19) can be integrated over  $y_N$  to give [16]

$$\frac{\partial f_{l-\bar{l}}}{\partial z} = -\frac{z^2 K}{2y_l^2} e^{-\frac{z^2+4y_l^2}{4y_l}} \left[ e^{y_l} f_{l-\bar{l}} - 2\varepsilon \left( \frac{n_N - n_N^{\text{eq}}}{n_N^{\text{eq}}} \right) \right]. \quad (3.20)$$

We further assume that both kinetic chemical equilibrium prevails for the leptons such that

$$\begin{aligned} f_{l-\bar{l}}^{\text{eq}} &= e^{-(E_l-\mu)/T} - e^{-(E_l+\mu)/T} \approx 2(\mu/T) e^{-E_l/T}, \\ n_{l-\bar{l}}^{\text{eq}} &\approx 2(\mu/T) n_l^{\text{eq}}, \\ f_{l-\bar{l}} &\approx \frac{n_{l-\bar{l}}}{n_l^{\text{eq}}} e^{-y_l}, \end{aligned} \quad (3.21)$$

with chemical potential  $\mu \ll 1$  and  $n_l^{\text{eq}}$  the lepton equilibrium number density. Thus, integrating over the lepton phase space, we obtain the equation of motion for the number density

$$\frac{\partial n_{l-\bar{l}}}{\partial z} = -\frac{z^3 K T^3}{2\pi^2} K_1(z) \left[ \frac{n_{l-\bar{l}}}{n_l^{\text{eq}}} - 2\varepsilon \left( \frac{n_N - n_N^{\text{eq}}}{n_N^{\text{eq}}} \right) \right], \quad (3.22)$$

where  $K_1(z)$  is the modified Bessel function of first kind. Following [7] we rewrite Eq. (3.22) in terms of the lepton asymmetry per co-moving photon ,

$$\frac{\partial N_{l-\bar{l}}}{\partial z} = -W_{ID} N_{l-\bar{l}} + \varepsilon D (N_N - N_N^{\text{eq}}), \quad (3.23)$$

where

$$W_{ID} \equiv \frac{1}{4} K z^3 K_1(z) = \frac{1}{2} D \frac{N_N^{\text{eq}}}{N_l^{\text{eq}}} \quad (3.24)$$

quantifies the strength of the wash-out due to inverse decays, and  $N_l^{\text{eq}} = 3/4$ . Note that, as with the RHN, when evaluating  $N_l^{\text{eq}}$  it is necessary to use a Fermi–Dirac distribution for the leptons,  $n_l^{\text{eq}} = (3/4)(\zeta(3)/\pi^2)g_l T^3$ , with  $g_l = 2$ , to ensure a realistic lepton to photon density ratio.

Figure 1 shows the final efficiency factor  $\kappa_f$ , defined in Eq. (2.8), as a function of  $K$  for several different initial RHN abundances [26].



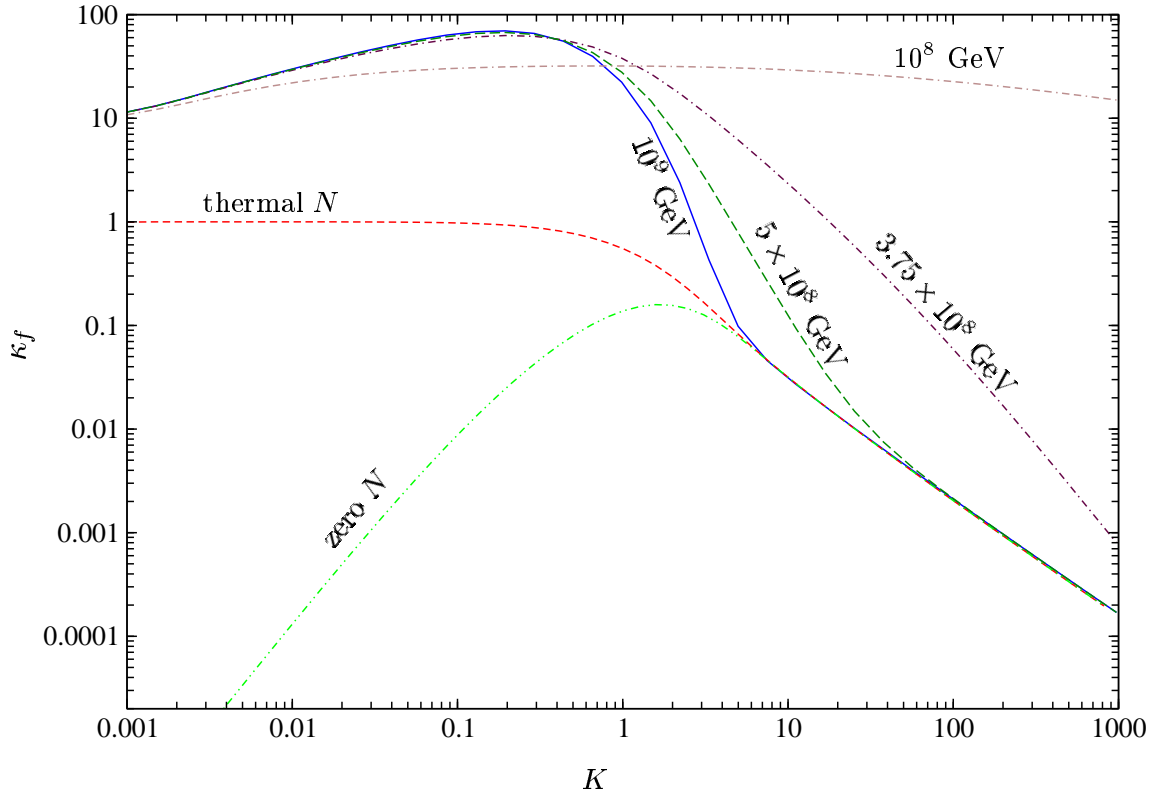


**Figure 1:** Final efficiency factor for different scenarios of thermal and non-thermal leptogenesis. Shown are  $\kappa_f$  for a thermal (dashed/red), a vanishing (dot-dot-dash/light green), and several cases of dominant initial RHN abundance. A dominant initial abundance is realized if a scalar field responsible for inflation decays exclusively into the RHN, which then dominates the energy density of the universe. The coupling strength between the scalar field and the RHN can be connected to an energy scale:  $10^9$  GeV (solid/blue),  $5 \times 10^8$  GeV (dashed/dark green),  $3.75 \times 10^8$  GeV (dot-dash/purple) and  $10^8$  GeV (dot-dash-dash/taupe).

### 3.2 Case D2: Dropping the assumption of kinetic equilibrium

Since the RHN is very heavy—its mass scale corresponds to the temperature of the thermal bath during the period of leptogenesis—it is not *a priori* obvious that decays and inverse decays would occur fast enough to establish kinetic equilibrium. Thus the assumption of kinetic equilibrium for the RHN might lead to sizable deviations from an exact treatment. In this section we drop this assumption in our calculation of the efficiency factor. We retain however our other assumptions: that all equilibrium distribution functions are of the Maxwell–Boltzmann form, and quantum statistical factors are negligible.

Dropping the assumption of kinetic equilibrium for the RHN means that it is now necessary to solve Eq. (3.14), rewritten here as

$$\frac{\partial f_N}{\partial z} = \frac{z^2 K}{\mathcal{E}_N} (e^{-\mathcal{E}_N} - f_N), \quad (3.25)$$

individually for all possible values of the dimensionless RHN energy  $\mathcal{E}_N$ . For the calculation of the

lepton asymmetry, the relevant equation is Eq. (3.19) which we reproduce here:

$$\frac{\partial f_{l-\bar{l}}}{\partial z} = -\frac{z^2 K}{2y_l^2} \int_{\frac{z^2-4y_l^2}{4y_l}}^{\infty} dy_N \frac{y_N}{\mathcal{E}_N} [f_{\Phi} f_{l-\bar{l}} - 2\varepsilon (f_N - f_N^{\text{eq}})]. \quad (3.26)$$

Again, this equation must be solved for all possible values of the lepton momentum  $y_l$ , and the resulting  $f_{l-\bar{l}}(y_l)$  summed according to Eq. (2.5) to give  $N_{l-\bar{l}}$ . Alternatively, using energy conservation and assuming kinetic and chemical equilibrium for the standard model particles, we can integrate Eq. (3.26) over the lepton phase space to obtain a single equation of motion for  $N_{l-\bar{l}}$ ,

$$\frac{\partial N_{l-\bar{l}}}{\partial z} = -\frac{z^2 K}{4} \int_0^{\infty} dy_l \int_{\frac{z^2-4y_l^2}{4y_l}}^{\infty} dy_N \frac{y_N}{\mathcal{E}_N} [N_{l-\bar{l}} f_N^{\text{eq}} - 2\varepsilon (f_N - f_N^{\text{eq}})]. \quad (3.27)$$

We find the second approach to yield more stable results.

### 3.3 Case D3: Boltzmann equations with quantum statistical factors

In Case D3 we reinstate Pauli blocking factors for fermions and factors due to induced emission for bosons, but adopt again the assumption of kinetic equilibrium for the RHN. Consistency requires that we use the Fermi–Dirac and the Bose–Einstein distribution functions respectively for fermions and bosons in thermal equilibrium, instead of the classical Maxwell–Boltzmann distribution function.

With these assumptions in mind, we integrate the collision integral (3.3) over  $p_{\Phi}$  to obtain the BE for the RHN,

$$\frac{\partial f_N}{\partial z} = \frac{z^2 K}{\mathcal{E}_N y_N} \frac{n_N - n_N^{\text{eq}}}{n_N^{\text{eq}}} \frac{1}{e^{\mathcal{E}_N} + 1} \log \left[ \frac{\sinh((\mathcal{E}_N - y_N)/2)}{\sinh((\mathcal{E}_N + y_N)/2)} \right], \quad (3.28)$$

where we have used  $f_N/f_N^{\text{eq}} = (1 + e^{\mathcal{E}_N})f_N \approx n_N/n_N^{\text{eq}}$ . Integrating over the RHN phase space and normalising to the photon number density yields

$$\frac{\partial N_N}{\partial z} = \frac{K}{K_2(z)} (N_N - N_N^{\text{eq}}) \int_0^{\infty} dy_N \frac{y_N}{\mathcal{E}_N} \frac{1}{e^{\mathcal{E}_N} + 1} \log \left[ \frac{\sinh((\mathcal{E}_N - y_N)/2)}{\sinh((\mathcal{E}_N + y_N)/2)} \right]. \quad (3.29)$$

We note that the integral over the RHN phase space has no simple analytic form. Therefore it remains necessary to perform the integration numerically.

The BE for the lepton asymmetry including all quantum statistical factors and assuming kinetic equilibrium for all particle species has the following form:

$$\frac{\partial f_{l-\bar{l}}}{\partial z} = -\frac{z^2 K}{2y_l^2} \int_{\frac{z^2-4y_l^2}{4y_l}}^{\infty} dy_N \frac{y_N}{\mathcal{E}_N} \left[ (f_{\Phi} + \frac{n_N}{n_N^{\text{eq}}} f_N^{\text{eq}}) (f_{l-\bar{l}} + \varepsilon F^+) - 2\varepsilon \frac{n_N}{n_N^{\text{eq}}} f_N^{\text{eq}} (1 + f_{\Phi}) \right], \quad (3.30)$$

where  $F^+ \equiv f_l + f_{\bar{l}} \approx 2f_l^{\text{eq}}$ . After integrating over the lepton phase space and normalising to the photon number density we arrive at

$$\begin{aligned} \frac{\partial N_{l-\bar{l}}}{\partial z} = & -\frac{z^2 K}{4} \int_0^{\infty} dy_l \\ & \times \int_{\frac{z^2-4y_l^2}{4y_l}}^{\infty} dy_N \frac{y_N}{\mathcal{E}_N} \left[ (f_{\Phi} + \frac{N_N}{N_N^{\text{eq}}} f_N^{\text{eq}}) \left( \frac{4}{3} N_{l-\bar{l}} + 2\varepsilon \right) f_l^{\text{eq}} - 2\varepsilon \frac{N_N}{N_N^{\text{eq}}} f_N^{\text{eq}} (1 + f_{\Phi}) \right], \end{aligned} \quad (3.31)$$

with  $N_N^{\text{eq}}$  given in Eq. (3.18).

### 3.4 Case D4: Complete mode equations

Here we include all statistical factors and make no assumption of kinetic equilibrium for the RHN. Integrating Eq. (3.3) over  $p_\Phi$  gives the BE for the RHN,

$$\frac{\partial f_N}{\partial z} = K \frac{z^2}{\mathcal{E}_N y_N} \frac{-1 + f_N + e^{\mathcal{E}_N} f_N}{e^{\mathcal{E}_N} + 1} \log \left[ \frac{\sinh((\mathcal{E}_N - y_N)/2)}{\sinh((\mathcal{E}_N + y_N)/2)} \right]. \quad (3.32)$$

The equation for the lepton asymmetry in this case is similar to Eq. (3.30), except we do not assume kinetic equilibrium for the RHN,

$$\frac{\partial f_{l-\bar{l}}}{\partial z} = -\frac{z^2 K}{2y_l^2} \int_{\frac{z^2 - 4y_l^2}{4y_l}}^{\infty} dy_N \frac{y_N}{\mathcal{E}_N} [(f_\Phi + f_N)(f_{l-\bar{l}} + \varepsilon F^+) - 2\varepsilon f_N (1 + f_\Phi)]. \quad (3.33)$$

Integrating over the RHN momentum yields

$$\begin{aligned} \frac{\partial N_{l-\bar{l}}}{\partial z} = & -\frac{z^2 K}{4} \int_0^\infty dy_l \\ & \times \int_{\frac{z^2 - 4y_l^2}{4y_l}}^{\infty} dy_N \frac{y_N}{\mathcal{E}_N} \left[ (f_\Phi + f_N) \left( \frac{4}{3} N_{l-\bar{l}} + 2\varepsilon \right) f_l^{\text{eq}} - 2\varepsilon f_N (1 + f_\Phi) \right], \end{aligned} \quad (3.34)$$

where we have assumed, as usual, thermal equilibrium for the standard model particles.

## 3.5 Results and discussions

### 3.5.1 Right-handed neutrino

Figure 2 shows the time evolution of the comoving number densities of the RHN for the four different cases described above, assuming a vanishing initial RHN abundance. We have picked two values for the decay parameter: (i)  $K = 0.1$ , lying in the weak wash-out regime, is shown on the left hand side, and (ii)  $K = 10$ , lying in the strong wash-out regime, is shown on the right hand side. For reference, we also plot the time evolution of the RHN equilibrium number density  $N_N^{\text{eq}}$ .

The general behaviour of the RHN abundance evolution is similar for all four cases. In the weak wash-out regime, there is a net production of RHN by inverse decays at high temperatures  $z < 1$ . At  $z \sim 4$ , the RHN abundance overshoots the equilibrium density and continues to grow until  $z \sim 5$ , when a net destruction of RHN by decays into  $l\Phi$  pairs begins to push its abundance slowly back down to the equilibrium value. Equilibrium is reached finally at  $z \sim 20$ , beyond which the RHN abundance falls off exponentially with  $z$ , as expected for all non-relativistic particle species in thermal equilibrium. Contrastingly, in the strong wash-out regime, the stronger coupling brings the RHN abundance to its equilibrium value already at  $z \sim 1$ . Its subsequent evolution is then simply governed by equilibrium statistics: at  $z \sim 4$  the RHN becomes nonrelativistic and hence its abundance is suppressed by  $\exp(-M/T)$ .

In both the weak and strong wash-out regimes, the difference between Cases D1 and D2, which exclude quantum statistical factors, and their counterparts Cases D3 and D4, which include quantum statistics, is most visible at  $z \lesssim 1$ . The RHN abundance is almost an order of magnitude larger in the latter two cases than in the former. This is because during the high temperature RHN production phase, using the correct Bose–Einstein equilibrium distribution function for the Higgs

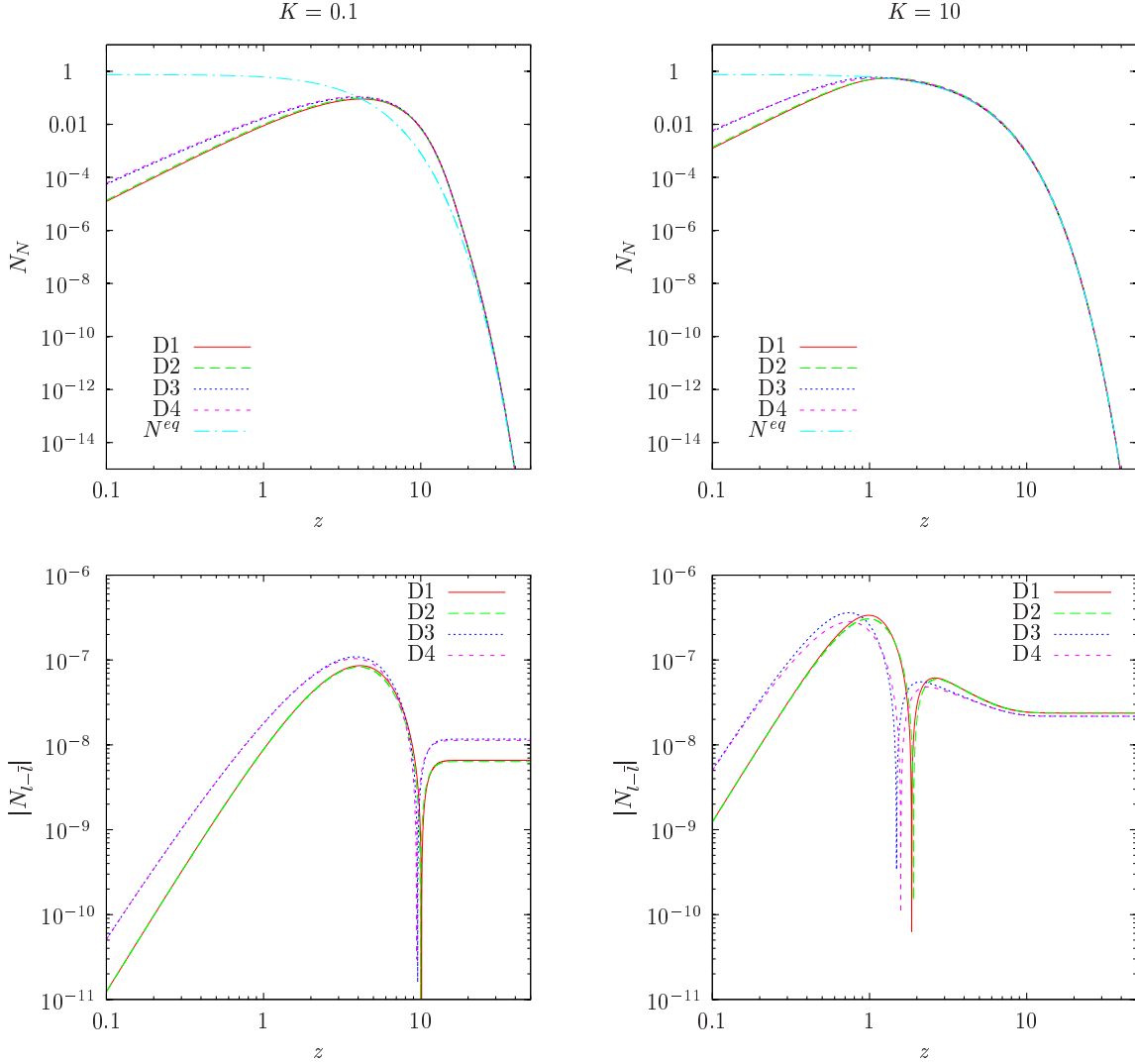


**Figure 2:** Time evolution of the comoving RHN number density  $N_N$  and of the absolute value of the lepton asymmetry  $N_{l-\bar{l}}$ , assuming two different coupling strengths  $K = 0.1, 10$ , and  $\varepsilon = 10^{-6}$ . The four scenarios within the decay–inverse decay only framework are shown: Solid/red line denotes Case D1, long dashed/green D2, dotted/blue D3, and short dashed/magenta D4. See table 1 for a short summary of each scenario. For reference, we also indicate the equilibrium RHN number density  $N_N^{eq}$  in dot-dash/cyan.

boson  $f_\Phi$  substantially enlarges the phase space available for the inverse decay process  $\Phi l \rightarrow N$  at low  $E_\Phi$ . This effect is far stronger than the phase space restriction due to Pauli blocking by the final state RHN, as can be seen from the phase space factors in Eq. (3.3). As the temperature drops and the RHN becomes nonrelativistic, the effects of quantum statistics also diminish, since kinematics now prevents the low energy  $\Phi$  and  $l$  states from contributing to the collision integrals.

Interestingly, the assumption of kinetic equilibrium leads to no visible effects in either the weak or strong wash-out regime. Comparing Cases D1 and D2 (both assume Maxwell–Boltzmann statistics), their RHN abundances are virtually identical. The same is true for Cases D3 and D4, which include quantum statistical factors.

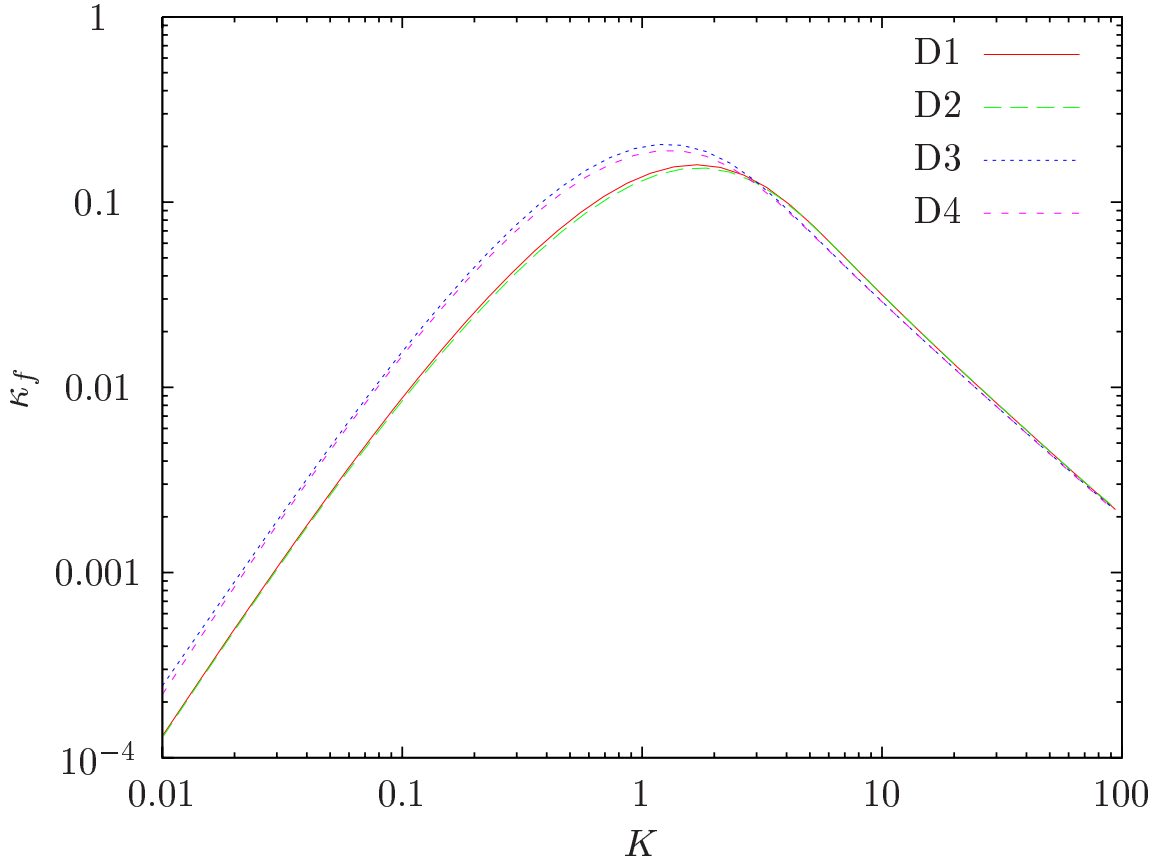


**Figure 3:** The final efficiency factor  $\kappa$  as a function of  $K$  for the four scenarios within the decay–inverse decay picture, assuming a vanishing initial RHN abundance. Solid/red line denotes Case D1, long dashed/green D2, dotted/blue D3, and short dashed/magenta D4.

### 3.5.2 Lepton asymmetry

The time evolution of the corresponding absolute value of the lepton asymmetry is shown in the lower panel of Figure 2. A negative lepton asymmetry is produced at high temperatures by RHN production from inverse decays. At  $z \sim 5$  in the weak wash-out regime ( $z \sim 1$  if strong wash-out), decays come to dominate over inverse decays, thus reversing the direction of the asymmetry production, and eventually flipping the sign of the asymmetry to positive. When the RHN abundance begins to fall off exponentially, the asymmetry also asymptotes to a final, constant value.

In the weak wash-out regime ( $K = 0.1$ ) the asymmetries produced in Cases D3 and D4 which include quantum statistical factors are always larger in magnitude than those produced in Cases D1 and D2 which assume Maxwell–Boltzmann statistics throughout the whole temperature range considered. The change of sign also occurs slightly earlier in D3 and D4. These effects can be understood as follows. From, e.g., Eq. (3.33), we see that the production of a negative lepton asymmetry at high temperatures by inverse RHN decays is significantly enhanced when we take proper account of the Bose–Einstein statistics for the Higgs boson. Like the case of the RHN abundance, this effect dominates over the phase space suppression due to the Fermi–Dirac statistics of the lepton and the RHN. As we progress to lower temperatures, RHN decays begin to

dominate over inverse decays, thereby reversing the direction of the lepton asymmetry evolution. Since quantum statistics speeds up RHN production and brings its abundance up to the equilibrium threshold earlier, the transition from decay to inverse decay domination—and hence the turning point in the asymmetry evolution—also happens earlier. As a result, the asymmetry flips sign a little earlier in Cases D3 and D4 than in D1 and D2, and has more time to grow to a larger positive value before the exponential fall-off of the RHN abundance shuts down the asymmetry production.

In the strong wash-out regime ( $K = 10$ ), a similar behaviour is also visible at  $z \lesssim 1$ . As we progress to lower temperatures, however, Cases D3 and D4 end up producing less asymmetry than Cases D1 and D2. This is because for  $K > 1$ , the wash-out rate plays a dominant role in determining the final asymmetry. Here, quantum statistics enlarges the phase space of the wash-out term from  $f_\Phi f_{l-\bar{l}}$  in Eq. (3.26) to  $(f_\Phi + f_N) f_{l-\bar{l}}$  in Eq. (3.33), thus forcing the lepton asymmetry to flip sign even earlier, and continuing on to dampen it to a slightly smaller positive value.

Again, as with the RHN, the assumption of kinetic equilibrium has virtually no effect on the asymmetry evolution: the differences between Cases D1 and D2, and between Cases D3 and D4 are generally at the percent level, too small to be visible in Figure 2.

Finally, Figure 3 summarises the lepton asymmetry produced in the four cases, in terms of the final efficiency factor  $\kappa_f$  defined in Eq. (2.8), as a function of the decay parameter  $K$ . For all values of  $K$  considered, the assumption of kinetic equilibrium can be seen to produce a minute ( $< 5\%$ ) difference in  $\kappa_f$  between Cases D1 and D2 and between Cases D3 and D4. Quantum statistics, on the other hand, has a generally stronger effect on the final lepton asymmetry. In the weak wash-out regime ( $K \lesssim 1$ ), inclusion of quantum statistical factors (Cases D3 and D4) enhances  $\kappa_f$  by a factor of  $\sim 1.5$  relative to Cases D1 and D2 which assume Maxwell–Boltzmann statistics. In the strong wash-out regime ( $K \gtrsim 1$ ), the effect of quantum statistics is to suppress  $\kappa_f$  by up to 20% at  $K \sim 10$ , but reduces to the percent level at  $K \sim 100$ .

#### 4. Scattering processes

In this section we enlarge our picture of thermal leptogenesis to include tree level scattering processes of the RHN with the top quark, e.g.,  $Nl \rightarrow qt$ , which are of  $\mathcal{O}(h_t^2 \lambda^2)$ . These interactions lead to an additional production channel for the RHN and contribute to the wash-out processes. Until now these scattering processes have only been considered using the integrated Boltzmann equations [6, 7]. Here we provide for the first time a solution of the full set of Boltzmann equations at the mode level.

We do not consider interactions with gauge bosons, nor include  $CP$  violation in  $2 \rightarrow 2$  or  $1(2) \rightarrow 3$  processes, which are of higher order in the Yukawa couplings.  $CP$  violation from these processes was considered in [9, 27, 28, 29], where it was shown that at high temperatures  $CP$  violation from scattering is the main source of lepton asymmetry production. However the final asymmetry depends also on the strength of the wash-out processes; It turns out that in the weak wash-out regime ( $K < 1$ )  $CP$  violation in the scattering processes tends to suppress the asymmetry production, while in the transition ( $K \simeq 1$ ) and strong ( $K > 1$ ) wash-out regimes its contribution is small to negligible.

**Table 2:** Scenarios including scattering with the top quark and their associated assumptions. Case S1 corresponds to the conventional integrated Boltzmann approach, while Case S2 involves solving the full set of Boltzmann equations at the mode level.

	Assumption of kinetic equilibrium	Including quantum statistics	Section
Case S1	Yes	No	4.1
Case S2	No	Yes	4.2

In the following we first recall the treatment of scattering processes in the integrated picture, before we proceed to write down the full set of mode equations including the relevant scattering terms. Table 2 summarises the assumptions of these two scenarios.

#### 4.1 Case S1: Scattering in the integrated picture

Analogous to Eqs. (3.16) and (3.23), the integrated Boltzmann equations including scattering take the following form [7],

$$\frac{\partial N_N}{\partial z} = - (D + S) (N_N - N_N^{\text{eq}}), \quad (4.1)$$

$$\frac{\partial N_{l-\bar{l}}}{\partial z} = -W N_{l-\bar{l}} + \varepsilon D (N_N - N_N^{\text{eq}}), \quad (4.2)$$

where  $S$  accounts for the production of RHN from scattering processes, and the wash-out rate  $W$  contains also a contribution from these processes. The scattering rate  $S$  itself consists of two terms,  $S = 2S_s + 4S_t$ , coming respectively from scattering in the  $s$ -channel and in the  $t$ -channel. One factor of 2 stems from contribution from processes involving anti-particles, and another factor of 2 in the  $t$ -channel term originates from the  $u$ -channel diagram.

In general, the scattering rates are defined as

$$S_{s,t} = \frac{\Gamma_{s,t}}{H z}, \quad (4.3)$$

where

$$\Gamma_{s,t} = \frac{M}{24 \zeta(3) g_N \pi^2} \frac{\mathcal{I}_{s,t}}{K_2(z) z^3}. \quad (4.4)$$

Note that an additional factor of  $4/(3) \zeta(3)$  appears in this definition compared to the definition of reference [7]. This is due to the Fermi–Dirac statistics used in our derivation. The quantity  $\mathcal{I}_{s,t}$  is an integral

$$\mathcal{I}_{s,t} = \int_{z^2}^{\infty} d\Psi \hat{\sigma}_{s,t}(\Psi) \sqrt{\Psi} K_1(\sqrt{\Psi}) \quad (4.5)$$

of the reduced cross-section  $\hat{\sigma}_{s,t}$ , given by [4]

$$\hat{\sigma}_{s,t} = \frac{3 h_t^2}{4 \pi} \frac{M \tilde{m}_1}{v^2} \chi_{s,t}(x), \quad (4.6)$$

where  $x = \Psi/z^2$ , and  $h_t = h_t(T)$  is the top Yukawa coupling, to be evaluated at the relevant energy scale (or temperature)  $T$  by solving the renormalisation group equation. See Appendix B.

The functions  $\chi_{s,t}(x)$  are defined as

$$\chi_s(x) = \left( \frac{x-1}{x} \right)^2, \quad (4.7)$$

$$\chi_t(x) = \frac{x-1}{x} \left[ \frac{x-2+2a_h}{x-1+a_h} + \frac{1-2a_h}{x-1} \log \left( \frac{x-1+a_h}{a_h} \right) \right], \quad (4.8)$$

where we have introduced  $a_h = m_\Phi/M$  as an infrared cut-off for the  $t$ -channel diagram, and  $m_\Phi$  is the mass of the Higgs boson which presumably receives contributions from interactions with the thermal bath, i.e., its value does not correspond to that potentially measured at the LHC. The value of  $m_\Phi$  can in principle be deduced from a thermal field theoretic treatment of leptogenesis, and the analysis of [6] found  $m_\Phi(T) \simeq 0.4T$ . However some open questions still remain and hence in the present work we prefer to adopt a value of  $a_h = 10^{-5}$ , used first by Luty in [30].

It is convenient to rewrite the  $s$ - and  $t$ -channel scattering rates  $S_{s,t}$  in terms of the functions  $f_{s,t}$  defined as

$$f_{s,t}(z) = \frac{\int_{z^2}^{\infty} d\Psi \chi_{s,t}(\Psi/z^2) \sqrt{\Psi} K_1(\sqrt{\Psi})}{z^2 K_2(z)}, \quad (4.9)$$

such that

$$S_{s,t} = \frac{K_s}{9\zeta(3)} f_{s,t}, \quad (4.10)$$

and the total scattering rate is given by

$$S = \frac{2K_s}{9\zeta(3)} (f_s(z) + 2f_t(z)), \quad (4.11)$$

where

$$K_s = \frac{\tilde{m}_1}{m_*^s}, \quad (4.12)$$

with  $\tilde{m}_1$  given by Eqs. (3.5), and [7]

$$m_*^s = \frac{4\pi^2}{9} \frac{g_N}{h_t^2} m_*, \quad (4.13)$$

where  $m_*$  is defined in in Eq. (3.6).

Since the scattering processes with the top quark change the lepton number by one unit, they contribute also to the wash-out of the asymmetry. The total wash-out rate is given by

$$W = W_{ID} + W_{\Delta L=1}, \quad (4.14)$$

where  $W_{ID}$  denotes the contribution from inverse decay defined in Eq. (3.24), and  $W_{\Delta L=1}$  from scattering in the  $s$ - and  $t$ -channels,

$$W_{\Delta L=1} = W_s + 2W_t, \quad (4.15)$$

with

$$W_s = \frac{N_N}{N_N^{\text{eq}}} \frac{\Gamma_s^l}{H z} = \frac{N_N^{\text{eq}}}{N_l^{\text{eq}}} \frac{N_N}{N_N^{\text{eq}}} S_s, \quad (4.16)$$



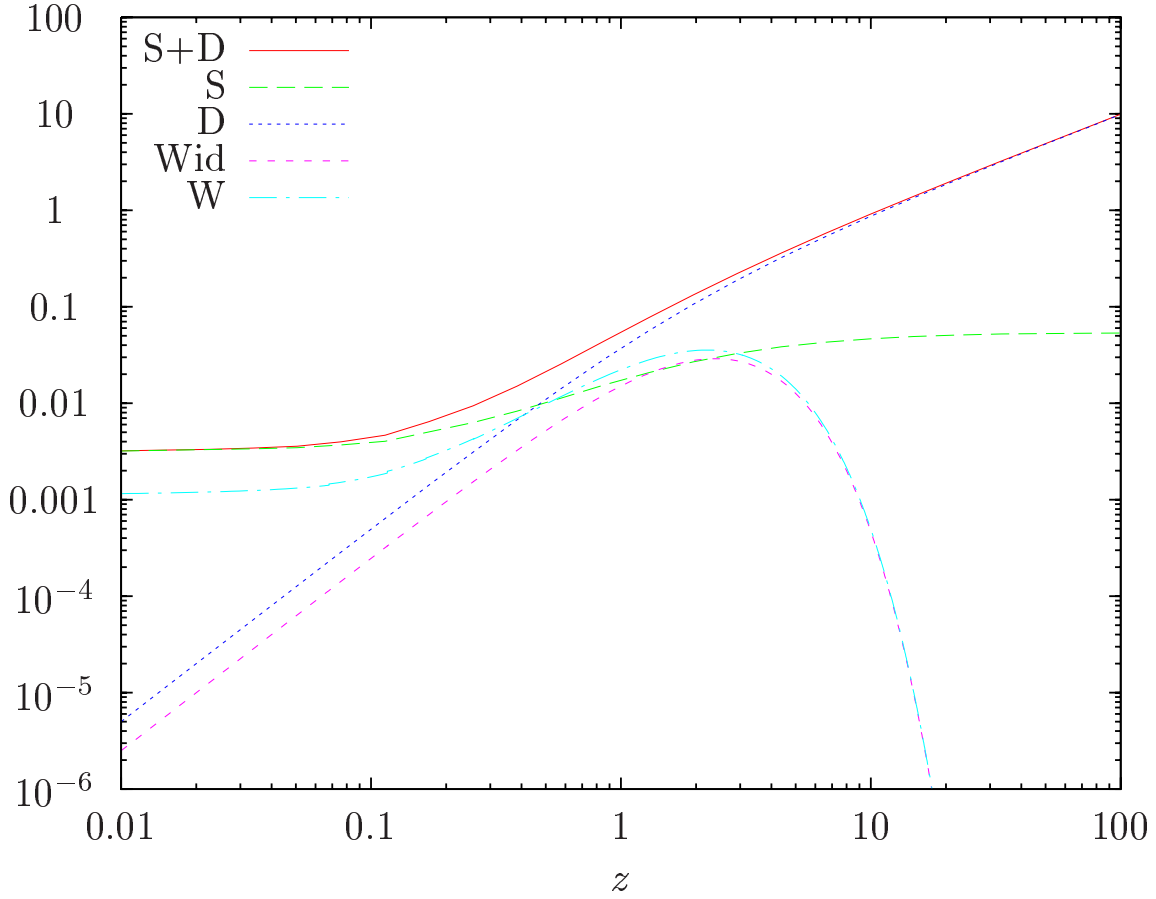


**Figure 4:** The decay  $D$ , scattering  $S$ , and wash-out rates  $W$  and  $W_{ID}$  as functions of  $z$  in the integrated approach, assuming  $K = 0.1$  and  $a_h = 10^{-5}$ .

and

$$W_t = \frac{\Gamma_t^l}{H z} = \frac{N_N^{\text{eq}}}{N_l^{\text{eq}}} S_t. \quad (4.17)$$

The lepton scattering rates are given by  $\Gamma_{s,t}^l = N_N^{\text{eq}}/N_l^{\text{eq}} \Gamma_{s,t}$ . Using Eq. (3.24), the two contributions  $W_{ID}$  and  $W_{\Delta L=1}$  are related by

$$W_{\Delta L=1} = 2 W_{ID} \frac{1}{D} \left( \frac{N_N}{N_N^{\text{eq}}} S_s + 2 S_t \right), \quad (4.18)$$

so that

$$W = W_{ID} \left[ 1 + \frac{1}{D} \left( 2 \frac{N_N}{N_N^{\text{eq}}} S_s + 4 S_t \right) \right] \quad (4.19)$$

gives the total wash-out rate.

Figure 4 shows the various rates  $D$ ,  $S$ ,  $W$  and  $W_{ID}$  as functions of  $z$  assuming  $K = 0.1$ . For other choices of  $K$ , the corresponding rates evolve with  $z$  in a similar fashion, but with magnitudes scaling with  $K$ .

## 4.2 Case S2: Complete mode equations including scattering

The basic BE for the distribution function of the RHN is given by

$$\frac{H(M)}{z} \frac{\partial f_N}{\partial z} = C_D [f_N] + 2 C_{S,s} [f_N] + 4 C_{S,t} [f_N], \quad (4.20)$$

where again one factor of 2 stems from contribution from processes involving anti-particles, and another factor of 2 in the  $t$ -channel term originates from the  $u$ -channel diagram. The decay–inverse decay collision integral  $C_D$  is given in Eq. (3.1), the  $s$ -channel scattering integral is

$$\begin{aligned} C_{S,s} [f_N] &= \frac{1}{2E_N} \int \prod_{i=l,q,t} \frac{dp_i^3}{(2\pi)^3 2E_i} (2\pi)^4 \delta^4(p_N + p_l - p_t - p_q) |\mathcal{M}_s|^2 \\ &\times [(1 - f_N)(1 - f_l) f_t f_q - f_N f_l (1 - f_t)(1 - f_q)], \end{aligned} \quad (4.21)$$

and a similar expression exists for the  $t$ -channel scattering integral  $C_{S,t} [f_N]$ , but with the appropriate matrix element  $\mathcal{M}_t$ , and the replacements  $f_l \leftrightarrow f_q$ .

The analogous equation for the lepton asymmetry is

$$\frac{H(M)}{z} \frac{\partial f_{l-\bar{l}}}{\partial z} = C_D [f_{l-\bar{l}}] + 2 C_{S,s} [f_{l-\bar{l}}] + 4 C_{S,t} [f_{l-\bar{l}}], \quad (4.22)$$

where  $C_D [f_{l-\bar{l}}] \equiv C_D [f_l] - C_D [f_{\bar{l}}]$  can be constructed from Eq. (3.8), and

$$\begin{aligned} C_{S,s} [f_{l-\bar{l}}] &= \frac{1}{2E_l} \int \prod_{i=N,q,t} \frac{dp_i^3}{(2\pi)^3 2E_i} (2\pi)^4 \delta^4(p_l + p_N - p_q - p_t) |\mathcal{M}_s|^2 \\ &\times f_{l-\bar{l}} (f_N (f_t + f_q - 1) - f_t f_q). \end{aligned} \quad (4.23)$$

Replacing  $\mathcal{M}_s$  with  $\mathcal{M}_t$  and  $f_q \leftrightarrow f_N$  in Eq. (4.23) yields the integral  $C_{S,t} [f_{l-\bar{l}}]$ .

The collision integrals (4.21) and (4.23) are nine-dimensional and can be reduced analytically down to two dimensions. We give in appendix A the final reduced integrals and, as an example, the full reduction procedure applied to the  $s$ -channel collisional integral for tracking the RHN following the method of [31, 32]. A general treatment of scattering kernels in kinetic equations can be found in [33].

## 4.3 Results and discussions

### 4.3.1 Scattering vs decay–inverse decay

Figure 5 shows snapshots of the RHN distribution function in Case S2 relative to an equilibrium Fermi–Dirac distribution at time  $z = 0.2, 1, 5$ , as well as the RHN number density normalised to its equilibrium value as a function of  $z$  for an interaction strength of  $K = 0.1$ . These are compared with their counterparts assuming decay and inverse decay only (Case D4). Figure 6 is similar, except for  $K = 10$ . Clearly, including scattering processes speeds up the equilibration of the RHN distribution function, especially at high temperatures ( $z < 1$ ). This effect is more significant for small values of  $K$ , since for large  $K$  values decays and inverse decays are already fast enough to establish equilibrium.

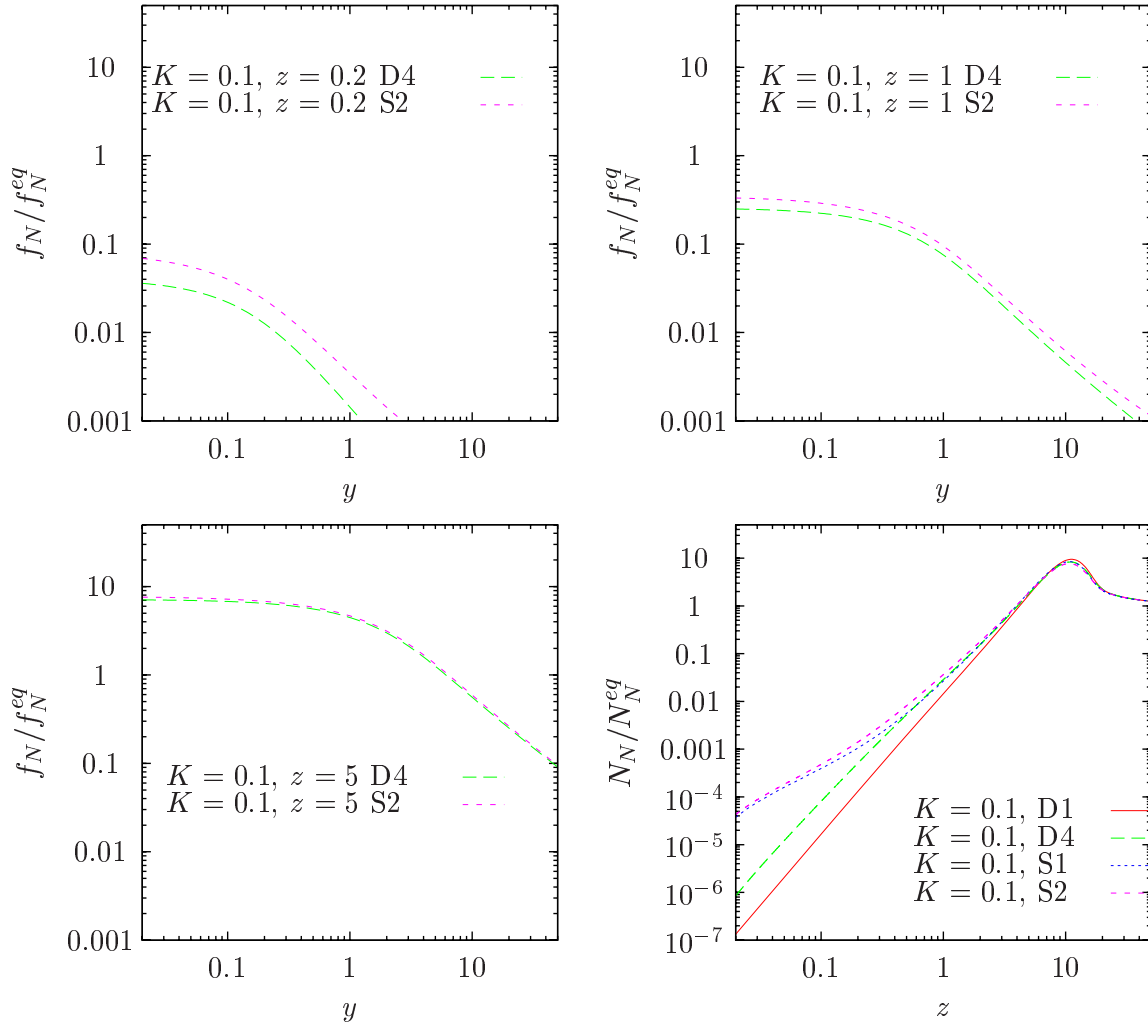


**Figure 5:** Snapshots of the RHN distribution function  $f_N/f_N^{eq}$  at  $z = 0.2, 1, 5$ , and the RHN abundance  $N_N/N_N^{eq}$  as a function of  $z$ , assuming  $K = 0.1$ . Solid/red line denotes Case D1, long dashed/green D4, dotted/blue S1, and short dashed/magenta S2. See tables 1 and 2 for a summary of the scenarios.

Looking at the time evolution of the RHN number density we see a corresponding increase in  $N_N$  at high temperatures when scattering is included (Case S2), compared to the case with decays and inverse decays only (Case D4). The equilibrium density is also reached at an earlier time (or higher temperature). The integrated approach shows a similar behaviour, with Case S1 predicting a large RHN abundance at high temperatures and hence faster equilibration than Case D1.

Figure 7 shows the time evolution of the lepton asymmetry, again for the two characteristic values of the decay parameter  $K = 0.1, 10$ . As discussed earlier, we have explicitly ignored  $CP$  violation in the scattering processes, so that they have no direct influence on the lepton asymmetry. This assumption is the reason why, in the weak wash-out regime ( $K = 0.1$ ), the asymmetry evolution at high temperatures ( $z < 1$ ) in Case S2 is virtually identical to that in its decay–inverse decay only counterpart Case D4. The same behaviour can also be seen when comparing Cases S1 and D1. Here, decays and inverse decays of the RHN alone source the creation of a lepton asymmetry.

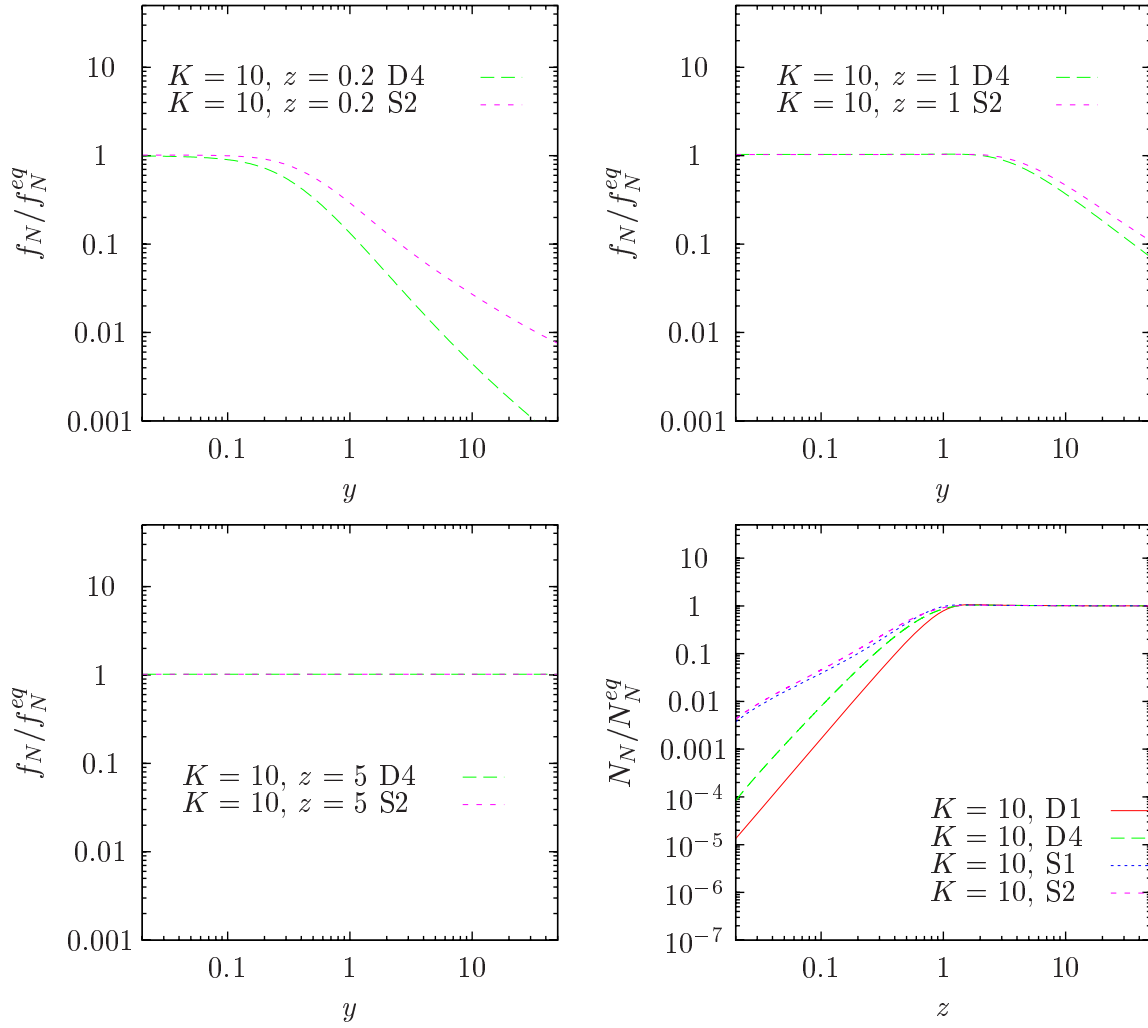


**Figure 6:** Same as Figure 5, but for  $K = 10$ .

Since for  $K < 1$  the asymmetry evolution at high temperatures hinges primarily on inverse decays and is as yet unaffected by such external factors as the RHN abundance and wash-out processes, the inclusion of scattering processes has no visible effect on  $N_{l-\bar{l}}$ .

However, scattering can still affect the asymmetry production in two indirect and competing ways: (i) the larger RHN abundance produced via scattering processes at high temperatures forces the lepton asymmetry to flip sign earlier, thereby generating a larger positive lepton asymmetry, and (ii) scattering leads to additional wash-out of the lepton asymmetry. The first effect dominates for coupling strengths lying in the weak wash-out regime ( $K < 1$ ), eventually leading to a larger asymmetry in Cases S1 and S2, compared with their decay–inverse decay only counterparts D1 and D4 as shown in Figure 7. For stronger couplings ( $K > 1$ ), the second effect dominates; in fact, Figure 7 shows that the additional wash-out due to scattering suppresses the lepton asymmetry production in Cases S1 and S2 already at high temperatures  $z < 1$ , compared with the decay–inverse decay only scenarios D1 and D4.

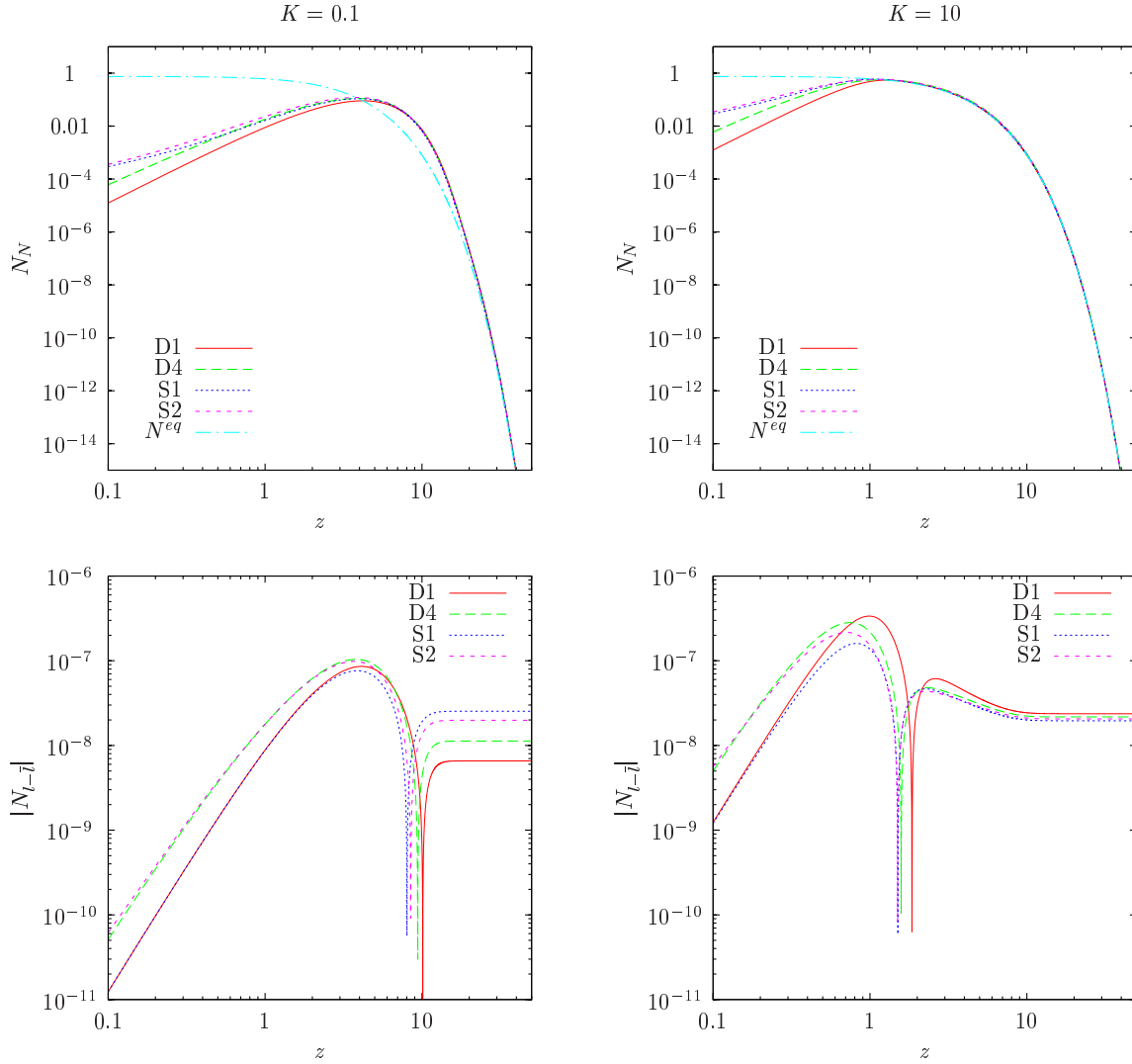


**Figure 7:** Time evolution of the absolute value of the lepton asymmetry  $|N_{l-\bar{l}}|$  for two different coupling strengths  $K$ . Shown are the two cases including scattering processes S1 (dotted/blue) and S2 (short dashed/magenta), and two scenarios D1 (solid/red) and D4 (long dashed/green) within the decays–inverse decay only framework. For reference we also plot the RHN equilibrium abundance (dot-dash/cyan).

### 4.3.2 Complete treatment vs integrated approach

The complete treatment differs from the integrated approach in that in the latter case we assume kinetic equilibrium for the RHN and neglect all quantum statistical factors. As we saw in section 3.5, the assumption of kinetic equilibrium tends to underestimate by a tiny amount the RHN abundance at  $z < 1$ . This can be understood from Figures 5 and 6 as a result of the more efficient production of low momentum RHN states, which in turn contribute more to the momentum integral.

Quantum statistics, on the other hand, has very different effects on the scattering and the decay–inverse decay collision terms. As we saw in section 3.5, in the decay–inverse decay scenario, quantum statistics always enhances the interaction rates through the enlarged Higgs boson phase space density  $f_\Phi$  at low  $E_\Phi$ . For the scattering processes, since all participants are fermions,

the role of quantum statistics is to reduce the phase space and hence suppress the interaction rates. In general, however, we expect quantum statistics to be more important for decay/inverse decay than for scattering. This is because in the decay–inverse decay case the enhanced phase space due to  $f_\Phi$  at low  $E_\Phi$  can in principle be infinite, while Pauli blocking for fermions participating in scattering, e.g.,  $1 - f_l$ , suppresses the phase space by at most a factor of  $1/2$ .

The difference between the RHN abundance and the lepton asymmetry evolution in the complete and the integrated treatments can then be understood in terms of a competition between the three aforementioned effects.

Consider first the RHN abundance. At  $z \ll 1$  the dominant RHN production channel is scattering. Here, suppression of the production rate due to quantum statistical factors competes with the small enhancement due to our dropping the assumption of kinetic equilibrium. The net result is that both Cases S1 and S2 give very similar RHN abundances as shown in Figures 5 to 7. At  $z \sim 0.3$ , decay/inverse decay becomes comparable to scattering (see Figure 4). Here, the enhanced decay rate due to quantum statistics in Case S2 pushes up RHN production relative to Case S1. This effect is more prominent in the weak wash-out regime than in the strong wash-out region, since in the former case the RHN abundance is further away from equilibrium. Progressing further in  $z$ , we see that the RHN abundances in Cases S1 and S2 become virtually identical already before reaching the equilibrium value. This is in stark contrast with the decay–inverse decay only scenarios, where the RHN abundances in Cases D1 and D4 clearly cross the equilibrium threshold at different times.

Consider now the evolution of the lepton asymmetry (lower panel of Figure 7). Comparing Cases S1 and S2 in the weak wash-out regime ( $K = 0.1$ ), quantum statistics in the latter scenario enhances the production of a negative lepton asymmetry at high temperatures. This effect is due solely to phase space enhancements in the inverse decay term, since we have assumed explicitly that scattering does not violate  $CP$ . At  $z \sim 4$ , the production of lepton asymmetry reverses direction as RHN decays begin to dominate over inverse decays. As mentioned earlier, quantum statistics causes this reversal to happen earlier in the decay–inverse decay only scenario by bringing the RHN abundance to the equilibrium threshold at an earlier time. When including scattering, however, the RHN abundances in both Cases S1 and S2 cross the equilibrium threshold at almost the same time, as discussed in the previous paragraph. This means that the evolution of their corresponding lepton asymmetries also turns around at roughly the same time. Since at the time of the turn-around Case S2 has a more negative asymmetry than Case S1, the net effect is that the asymmetry in Case S2 flips sign at a slightly later time than in Case S1, and subsequently grows to a smaller positive value.

The effects of quantum statistics on the lepton asymmetry evolution in the strong wash-out regime ( $K = 10$ ) can be similarly understood, except that we must consider also the role of the wash-out terms. At  $z \lesssim 1$ , the wash-out rate is dominated by scattering. However, as shown in Figure 4, decay/inverse decay becomes comparable to scattering at  $z \sim 0.3$  and is the dominant wash-out process at  $z \gtrsim 1$ . Thus, from  $z \sim 1$  onwards, the net effect of quantum statistics is to enhance the wash-out rate. This effect can be seen at the turn-around of the lepton asymmetry evolution: the stronger wash-out rate in Case S2 forces the lepton asymmetry evolution to reverse direction at a slightly earlier time than in Case S1. However, since at the time of the turn-around Case S2 has a more negative asymmetry than S1, the asymmetries in both cases end up flipping

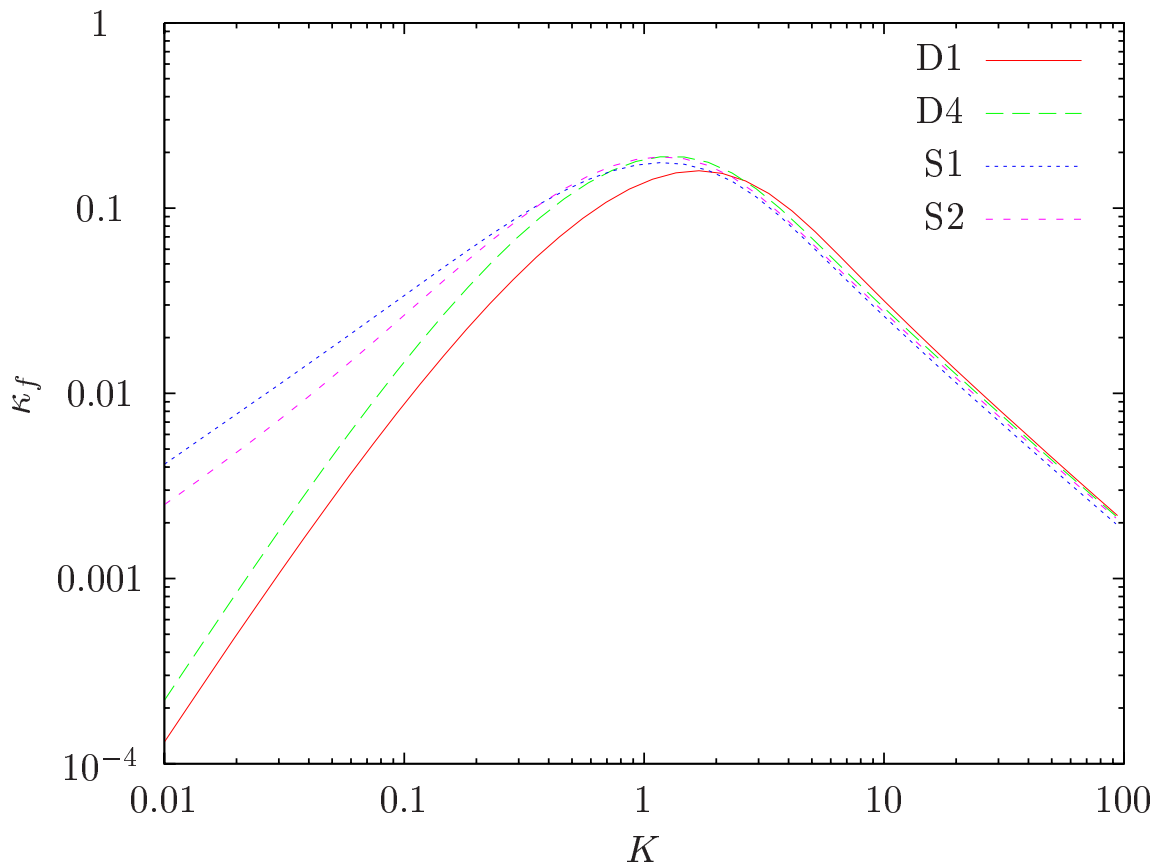


**Figure 8:** The final efficiency factor  $\kappa_f$  without and with scattering terms: D1 (solid), D4 (long dashed), S1 (dotted), and S2 (short dashed).

signs at almost the same time and grow to nearly identical values.

Finally, Figure 8 shows the final efficiency factors as a function of  $K$  for the integrated approach and the complete mode treatment, both including and excluding scattering. For Cases S1 and S2 which include scattering, we note that their difference is rather large in the weak wash-out regime ( $K < 1$ ), with the integrated approach overestimating  $\kappa_f$  by up to a factor  $\sim 1.5$  at  $K \sim 0.01$  compared to solving the complete mode equations. But this difference decreases as we increase  $K$ . At  $K \gtrsim 3$  the integrated approach underestimates  $\kappa_f$  by less than  $\sim 10\%$ .

It is also interesting to note that the relative contribution of scattering processes to the final efficiency factor is smaller in the complete mode calculation than in the integrated approach. In the weak wash-out regime, including scattering enhances the final efficiency factor from decays and inverse decays by up to a factor of  $\sim 30$  in the integrated scenario. In the complete mode calculation, however, the enhancement is only a factor of  $\sim 15$ . Similarly, in the strong wash-out regime, scattering reduces  $\kappa_f$  by up to 20% in the integrated picture, compared to below 10% in the complete treatment.

## 5. Conclusions

In this paper we have for the first time studied leptogenesis by means of the full Boltzmann equa-

tions incorporating all quantum statistical terms without the assumption of kinetic equilibrium, and including scatterings of the right-handed neutrino with quarks. This is of particular relevance for the creation of the cosmological baryon asymmetry due to the required deviation from thermal equilibrium and the energy dependence of all interactions. As the simplest possible set-up to study these effects, we have considered only an asymmetry being created by the lightest right-handed neutrino and have neglected potentially important flavour effects.

In the conventional approach, i.e., neglecting quantum statistical factors and assuming kinetic equilibrium, considering only decays and inverse decays is known to give a rather precise approximation of the final baryon asymmetry in the interesting strong wash-out regime. Hence, we start by considering this case, which also offers the possibility to study the influence of various effects separately and in detail.

Interestingly enough, dropping the assumption of kinetic equilibrium has almost no effect on the evolution of the RHN number density and the lepton asymmetry. Taking the full energy dependence of interactions into account changes the final efficiency factor by 5% at the most.

Including all quantum statistical factors has somewhat larger effects. These factors tend to enlarge the phase space available for neutrino production by inverse decays, thus significantly boosting the RHN abundance and the “wrong-sign” asymmetry being produced at high temperatures. Further, they lead to an earlier domination of decays over inverse decays, thus speeding up the production of the final asymmetry. In the weak wash-out regime this leaves more time for the production of an asymmetry, thus leading to a boost in the final asymmetry by  $\sim 50\%$ .

In the strong wash-out regime, on the other hand, the final asymmetry is suppressed by between 20% at  $K = 10$  and 1% at  $K = 100$ . This is again due to the enlarged phase space of inverse decay processes which act as wash-out terms, thus reducing the asymmetry compared to the case where quantum statistical factors are neglected.

In the case of scatterings of RHNs off quarks, in contrast to decays and inverse decays, quantum statistical factors reduce the phase space available, since all external particles in these processes are fermions. Hence, quantum effects generally tend to reduce the importance of these scatterings.

Nonetheless, at high temperatures ( $z < 1$ ) scattering processes increase the amount of RHNs being produced, thus making leptogenesis more efficient. On the other hand, at low temperatures ( $z > 1$ ) they act as wash-out terms thereby reducing the produced asymmetry. The first effect, i.e., the more efficient production of RHNs dominates in the weak wash-out regime, thus leading to a larger final lepton asymmetry compared to the case where only decays and inverse decays are included. In the strong wash-out regime the effect from increased wash-out dominates, i.e., including scatterings leads to a somewhat reduced asymmetry here.

This is qualitatively in line with results obtained in the integrated picture, i.e., neglecting quantum statistical factors and assuming kinetic equilibrium. However, since quantum statistical factor enhance decays and inverse decays while suppressing scatterings of RHNs with quarks, the net influence of these scattering processes is reduced when quantum factors are included. This significantly reduces the spread of results for the final efficiency factor, particularly in the weak wash-out regime.



## Acknowledgments

We thank Steen Hannestad, Josef Pradler, Max Huber and Georg Raffelt for useful discussions.

## Appendices

### A. Reduction of the scattering collision integrals

#### A.1 $s$ -channel

##### A.1.1 Right-handed neutrino

The full collision term for the  $s$ -channel in Eq. (4.20) is

$$C_{S,s}[f_N] = \frac{1}{2E_N} \int \prod_{i=l,q,t} \frac{d^3 p_i}{(2\pi)^3 2E_i} (2\pi)^4 \delta^4(p_N + p_l - p_t - p_q) |\mathcal{M}_s|^2 \Lambda_s^{(N)}(f_N, f_l, f_t, f_q), \quad (\text{A.1})$$

with phase space factor  $\Lambda_s^{(N)}$  given by

$$\Lambda_s^{(N)}(f_N, f_l, f_t, f_q) = [(1 - f_N)(1 - f_l)f_t f_q - f_N f_l(1 - f_t)(1 - f_q)]. \quad (\text{A.2})$$

The matrix element  $\mathcal{M}_s$  is summed over all internal degrees of freedom of the particles in the initial and final states, including colour and isospin, and is given by

$$|\mathcal{M}_s|^2 = 24 h_t^2 \frac{M \tilde{m}_1}{v^2} \frac{p_N p_l p_t p_q}{s^2}, \quad (\text{A.3})$$

where  $\tilde{m}_1 = (m_D^\dagger m_D) / M$  is the effective neutrino mass [20],  $v = 174$  GeV the vacuum expectation value of the Higgs field and  $h_t^2$  the top Yukawa coupling given in Appendix B.

We work in the centre-of-mass frame, i.e.,

$$\mathbf{p}_N + \mathbf{p}_l = \mathbf{p}_t + \mathbf{p}_q \equiv \mathbf{q}. \quad (\text{A.4})$$

In general, the 4-vector delta function can be dealt with using the relation

$$\begin{aligned} \delta(p_i^2 - M_i^2) &= \delta(E_i^2 - (|\mathbf{p}_i|^2 + M_i^2)) \\ &= \left( \frac{\delta(E_i - \sqrt{|\mathbf{p}_i|^2 + M_i^2})}{2\sqrt{|\mathbf{p}_i|^2 + M_i^2}} + \frac{\delta(E_i + \sqrt{|\mathbf{p}_i|^2 + M_i^2})}{2\sqrt{|\mathbf{p}_i|^2 + M_i^2}} \right). \end{aligned} \quad (\text{A.5})$$

Using this relation, and the fact that we consider all particles except the RHN to be massless, i.e.,

$$\begin{aligned} E_{l,t,q} &= |\mathbf{p}_{l,t,q}|, \\ E_N &= \sqrt{|\mathbf{p}_N|^2 + M^2}, \end{aligned} \quad (\text{A.6})$$

we can integrate over the quark energy,

$$\begin{aligned}
\int \frac{d^3 p_q}{2E_q} \delta^4(p_N + p_l - p_t - p_q) &= \int dE_q d^3 p_q \frac{\delta(E_q - |\mathbf{p}_q|)}{2|\mathbf{p}_q|} \Theta(E_q) \delta(E_N + E_l - E_t - E_q) \\
&\quad \times \delta^3(\mathbf{p}_N + \mathbf{p}_l - \mathbf{p}_t - \mathbf{p}_q) \\
&= \frac{\delta(E_N + E_l - E_t - |\mathbf{p}_N + \mathbf{p}_l - \mathbf{p}_t|)}{2|\mathbf{p}_N + \mathbf{p}_l - \mathbf{p}_t|} \Theta(E_N + E_l - E_t) \\
&= \frac{\delta(E_N + E_l - E_t - |\mathbf{q} - \mathbf{p}_t|)}{2|\mathbf{q} - \mathbf{p}_t|} \Theta(E_N + E_l - E_t) \\
&= \delta((E_N + E_l - E_t)^2 - |\mathbf{q} - \mathbf{p}_t|^2) \Theta(E_N + E_l - E_t).
\end{aligned} \tag{A.7}$$

Similarly, we can rewrite

$$\begin{aligned}
\frac{d^3 p_l}{2E_l} &= \int dE_l \frac{\delta(E_l - |\mathbf{p}_l|)}{2|\mathbf{p}_l|} \Theta(E_l) d^3 p_l \\
&= \int dE_l \delta(E_l^2 - |\mathbf{p}_l|^2) \Theta(E_l) d^3 p_l \\
&= \int dE_l \delta(E_l^2 - |\mathbf{q} - \mathbf{p}_N|^2) \Theta(E_l) d^3 q,
\end{aligned} \tag{A.8}$$

where the last equality follows from changing the variable from  $\mathbf{p}_l$  to  $\mathbf{q} = \mathbf{p}_N + \mathbf{p}_l$ , and hence  $d^3 p_l$  to  $d^3 q$ , and the integration is over the lepton energy  $E_l$ .

We choose an explicit coordinate system,

$$\begin{aligned}
\mathbf{q} &= |\mathbf{q}| (0, 0, 1), \\
\mathbf{p}_N &= |\mathbf{p}_N| (0, \sin \eta, \cos \eta), \\
\mathbf{p}_t &= E_t (\cos \phi \sin \vartheta, \sin \phi \sin \vartheta, \cos \vartheta),
\end{aligned} \tag{A.9}$$

and obtain the following quantities:

$$\begin{aligned}
s &= (p_N + p_l)^2 = (p_t + p_q)^2 = (E_N + E_l)^2 - |\mathbf{q}|^2, \\
p_N p_l &= \frac{s - M^2}{2}, \\
p_q p_t &= \frac{s}{2}, \\
|\mathbf{q} - \mathbf{p}_t|^2 &= |\mathbf{q}|^2 + |\mathbf{p}_t|^2 - 2\mathbf{q} \cdot \mathbf{p}_t = |\mathbf{q}|^2 + E_t^2 - 2|\mathbf{q}| E_t \cos \vartheta, \\
|\mathbf{q} - \mathbf{p}_N|^2 &= |\mathbf{q}|^2 + |\mathbf{p}_N|^2 - 2\mathbf{q} \cdot \mathbf{p}_N = |\mathbf{q}|^2 + |\mathbf{p}_N|^2 - 2|\mathbf{q}| |\mathbf{p}_N| \cos \eta.
\end{aligned} \tag{A.10}$$

The matrix element in these coordinates reads

$$|\mathcal{M}_s|^2 = 6 h_t^2 \frac{M \tilde{m}_1}{v^2} \frac{(E_N + E_l)^2 - M^2 - |\mathbf{q}|^2}{(E_N + E_l)^2 - |\mathbf{q}|^2}, \tag{A.11}$$

and the delta functions are given by

$$\begin{aligned}
\delta\left((E_N + E_l - E_t)^2 - |\mathbf{q} - \mathbf{p}_t|^2\right) &= \delta\left((E_N + E_l - E_t)^2 - |\mathbf{q}|^2 - E_t^2 + 2|\mathbf{q}| E_t \cos \vartheta\right) \\
&= \frac{1}{2|\mathbf{q}| E_t} \delta\left(\cos \vartheta - \frac{E_t^2 - (E_N + E_l - E_t)^2 + |\mathbf{q}|^2}{2|\mathbf{q}| E_t}\right), \\
\delta\left(E_l^2 - |\mathbf{q} - \mathbf{p}_N|^2\right) &= \delta\left(E_l^2 - |\mathbf{q}|^2 - |\mathbf{p}_N|^2 + 2|\mathbf{q}||\mathbf{p}_N| \cos \eta\right) \\
&= \frac{1}{2|\mathbf{q}||\mathbf{p}_N|} \delta\left(\cos \eta - \frac{|\mathbf{p}_N|^2 - E_l^2 + |\mathbf{q}|^2}{2|\mathbf{q}||\mathbf{p}_N|}\right).
\end{aligned} \tag{A.12}$$

Collecting all terms we get for the collision integral

$$\begin{aligned}
C_{S,s}[f_N] &= \frac{1}{2 E_N (2\pi)^5} \int \frac{d\Omega_N}{4\pi} d \cos \vartheta d\phi \frac{E_t^2}{2E_t} dE_t dE_l d^3q \frac{1}{2|\mathbf{q}||\mathbf{p}_N|} \frac{1}{2|\mathbf{q}| E_t} |\mathcal{M}_s|^2 \\
&\quad \times \delta\left(\cos \eta - \frac{|\mathbf{p}_N|^2 - E_l^2 + |\mathbf{q}|^2}{2|\mathbf{q}||\mathbf{p}_N|}\right) \delta\left(\cos \vartheta - \frac{E_t^2 - (E_l + E_N - E_t)^2 + |\mathbf{q}|^2}{2|\mathbf{q}| E_t}\right) \\
&\quad \times \Lambda_s^{(N)}(f_N, f_l, f_t, f_q) \Theta(E_l) \Theta(E_t) \Theta(E_l + E_N - E_t) \\
&= \frac{1}{2^7 \pi^3 E_N |\mathbf{p}_N|} \int d \cos \vartheta d \cos \eta dE_t dE_l d|\mathbf{q}| |\mathcal{M}_s|^2 \\
&\quad \times \delta\left(\cos \eta - \frac{|\mathbf{p}_N|^2 - E_l^2 + |\mathbf{q}|^2}{2|\mathbf{q}||\mathbf{p}_N|}\right) \delta\left(\cos \vartheta - \frac{E_t^2 - (E_l + E_N - E_t)^2 + |\mathbf{q}|^2}{2|\mathbf{q}| E_t}\right) \\
&\quad \times \Lambda_s^{(N)}(f_N, f_l, f_t, f_q) \Theta(E_l) \Theta(E_t) \Theta(E_l + E_N - E_t).
\end{aligned} \tag{A.13}$$

Here, in the first equality, we take  $d^3p_t = E_t^2 dE_t d \cos \vartheta d\phi$ , and average over the direction of the incoming RHN by integrating over  $d\Omega_N/(4\pi)$ , where  $d\Omega_N = d\theta d \cos \eta$ , because of rotational invariance (cf. Eq (A.9)). In the second equality, we take  $d^3q = 4\pi |\mathbf{q}|^2 d|\mathbf{q}|$ , and integrate over all azimuthal angles.

The two remaining angles  $\vartheta$  and  $\eta$  run in the range

$$\cos \vartheta, \cos \eta \in [-1, 1]. \tag{A.14}$$

Since apart from the delta functions the integrand does not depend on either angle, integrating over these ranges effectively lead to new integration limits for the  $q$ -integral:

$$\begin{aligned}
\cos \vartheta = 1 &\Rightarrow q \in [E_l + E_N, -E_l - E_N + 2E_t], \\
\cos \vartheta = -1 &\Rightarrow q \in [-E_l - E_N, E_l + E_N - 2E_t], \\
\cos \eta = 1 &\Rightarrow q \in [-E_l + p_N, E_l + p_N], \\
\cos \eta = -1 &\Rightarrow q \in [-E_l - p_N, E_l - p_N],
\end{aligned} \tag{A.15}$$

where  $p_N \equiv |\mathbf{p}_N|$ , and  $q \equiv |\mathbf{q}|$ . Putting these conditions together we get

$$\sup[|2E_t - E_l - E_N|, |E_l - p_N|] \leq q \leq \inf[E_l + E_N, E_l + p_N]. \tag{A.16}$$

Since  $E_l + E_N > E_l + p_N$  this reduces to

$$\sup[|2E_t - E_l - E_N|, |E_l - p_N|] \leq q \leq E_l + p_N. \tag{A.17}$$

Thus, the integration over  $\cos \eta$  and  $\cos \vartheta$  effectively gives rise to a combination of  $\Theta$  functions in the remaining 3-dimensional integral. Together with existing  $\Theta$  functions in Eq. (A.13), we define

$$\Omega \equiv \Theta(q - |2E_t - E_l - E_N|) \Theta(q - |E_l - p_N|) \Theta(E_l + p_N - q) \Theta(E_l + E_N - E_t) \quad (\text{A.18})$$

to collectively denote all  $\Theta$  functions appearing in the remaining integral. Note that we have omitted writing out  $\Theta(E_l)\Theta(E_t)$ , since positive particle energies are understood.

Next, we use the relations

$$\Theta(q - |2E_t - E_l - E_N|) = 1 - \Theta(|2E_t - E_l - E_N| - q), \quad (\text{A.19})$$

and

$$\Theta(|2E_t - E_l - E_N| - q) \Theta(E_l + p_N - q) = \Theta(|2E_t - E_l - E_N| - q), \quad (\text{A.20})$$

the latter following from the fact that  $\Omega$  in Eq. (A.18) vanishes unless  $|2E_t - E_l - E_N| < E_l + p_N$ . With these we split the function  $\Omega$  into two parts (i.e.,  $\Omega = \Omega_1 + \Omega_2$ ):

$$\Omega_1 = \Theta(E_l + E_N - E_t) \Theta(q - |E_l - p_N|) \Theta(E_l + p_N - q), \quad (\text{A.21})$$

$$\Omega_2 = -\Theta(E_l + E_N - E_t) \Theta(q - |E_l - p_N|) \Theta(|2E_t - E_l - E_N| - q). \quad (\text{A.22})$$

Equation (A.21) can be further split into two parts at  $\Theta(q - |E_l - p_N|)$  using the relation

$$\Theta(E_l - p_N) + \Theta(p_N - E_l) = 1, \quad (\text{A.23})$$

from which we find

$$\Omega_{1a} = \Theta(E_l + E_N - E_t) \Theta(q - (E_l - p_N)) \Theta(E_l + p_N - q) \Theta(E_l - p_N), \quad (\text{A.24})$$

$$\Omega_{1b} = \Theta(E_l + E_N - E_t) \Theta(q - (p_N - E_l)) \Theta(E_l + p_N - q) \Theta(p_N - E_l), \quad (\text{A.25})$$

so that  $\Omega_1 = \Omega_{1a} + \Omega_{1b}$ .

Similarly, Eq. (A.22) can be split at  $\Theta(q - |E_l - p_N|)$  into two parts,  $\Omega_2 = \Omega_{2a} + \Omega_{2b}$ , by way of the relation (A.23):

$$\Omega_{2a} = -\Theta(E_l + E_N - E_t) \Theta(q - (E_l - p_N)) \Theta(|2E_t - E_l - E_N| - q) \Theta(E_l - p_N), \quad (\text{A.26})$$

$$\Omega_{2b} = -\Theta(E_l + E_N - E_t) \Theta(q - (p_N - E_l)) \Theta(|2E_t - E_l - E_N| - q) \Theta(p_N - E_l). \quad (\text{A.27})$$

One further split is possible at  $\Theta(|2E_t - E_l - E_N| - q)$  using

$$\Theta(E_l + E_N - 2E_t) + \Theta(2E_t - E_l - E_N) = 1. \quad (\text{A.28})$$

Putting this relation in Eqs. (A.26) and (A.27), we find the combinations

$$\begin{aligned} \Theta(q - (E_l - p_N)) \Theta(E_l + E_N - 2E_t - q) &\Rightarrow E_t \leq \frac{1}{2}(E_N + p_N), \\ \Theta(q - (E_l - p_N)) \Theta(2E_t - E_l - E_N - q) &\Rightarrow E_t \geq \frac{1}{2}(2E_l + (E_N - p_N)), \\ \Theta(q - (p_N - E_l)) \Theta(E_l + E_N - 2E_t - q) &\Rightarrow E_t \leq \frac{1}{2}(2E_l + (E_N - p_N)), \\ \Theta(q - (p_N - E_l)) \Theta(2E_t - E_N - E_l - q) &\Rightarrow E_t \geq \frac{1}{2}(E_N + p_N), \end{aligned} \quad (\text{A.29})$$

with which we can write down the four parts of  $\Omega_2$ :

$$\begin{aligned}\Omega_{2a,i} &= -\Theta\left(\frac{1}{2}(E_N + p_N) - E_t\right) \Theta(q - (E_l - p_N)) \Theta(E_l + E_N - 2E_t - q) \\ &\quad \times \Theta(E_l - p_N),\end{aligned}\tag{A.30}$$

$$\begin{aligned}\Omega_{2a,ii} &= -\Theta(E_l + E_N - E_t) \Theta\left(E_t - \frac{1}{2}(2E_l + E_N - p_N)\right) \Theta(2E_t - E_l - E_N - q) \\ &\quad \times \Theta(q - (E_l - p_N)) \Theta(E_l - p_N),\end{aligned}\tag{A.31}$$

$$\begin{aligned}\Omega_{2b,i} &= -\Theta\left(\frac{1}{2}(2E_l + E_N - p_N) - E_t\right) \Theta(E_l + E_N - 2E_t - q) \\ &\quad \times \Theta(q - (p_N - E_l)) \Theta(p_N - E_l),\end{aligned}\tag{A.32}$$

$$\begin{aligned}\Omega_{2b,ii} &= -\Theta(E_l + E_N - E_t) \Theta\left(E_t - \frac{1}{2}(E_N + p_N)\right) \Theta(2E_t - E_l - E_N - q) \\ &\quad \times \Theta(q - (p_N - E_l)) \Theta(p_N - E_l),\end{aligned}\tag{A.33}$$

such that  $\Omega_{2a} = \Omega_{2a,i} + \Omega_{2a,ii}$  and  $\Omega_{2b} = \Omega_{2b,i} + \Omega_{2b,ii}$ .

Finally, collecting all terms we obtain the relation

$$\Omega = \sum_{\mu} \Omega_{\mu} = \Omega_{1a} + \Omega_{1b} + \Omega_{2a,i} + \Omega_{2a,ii} + \Omega_{2b,i} + \Omega_{2b,ii},\tag{A.34}$$

so that the remaining 3-dimensional integration in the collision integral (A.13) can be equivalently written as

$$C_{S,s}[f_N] = \sum_{\mu} \frac{1}{2^7 \pi^3 E_N |\mathbf{p}_N|} \int dE_t dE_l dq |\mathcal{M}_s|^2 \Lambda_s^{(N)}(f_N, f_l, f_t, f_q) \Omega_{\mu}.\tag{A.35}$$

The phase space factor reads

$$\Lambda_s^{(N)}(f_N, f_l, f_t, f_q) = -\frac{e^{\mathcal{E}_l + \mathcal{E}_t} (-1 + f_N + e^{\mathcal{E}_N} f_N)}{(1 + e^{\mathcal{E}_l}) (1 + e^{\mathcal{E}_t}) (e^{\mathcal{E}_l + \mathcal{E}_N} + e^{\mathcal{E}_t})},\tag{A.36}$$

where we have used energy conservation, and Fermi–Dirac statistics for the leptons and quarks.

The integration over  $q$  can now be performed analytically, reducing the dimensions of the collision integrals to two. These final integrals must be evaluated numerically and then summed to give  $C_{S,s}[f_N]$ ,

$$C_{S,s}[f_N] = C_s^{(1)} + C_s^{(2)} + C_s^{(3)} + C_s^{(4)} + C_s^{(5)} + C_s^{(6)}.\tag{A.37}$$

The integrals  $C_{S,s}^{(1,\dots,6)}$  are as follows:

- The first integral comes from evaluating the  $\Theta$  function  $\Omega_{1a}$ , and we have defined  $\tilde{q} \equiv q/T$ :

$$C_{S,s}^{(1)} = \frac{3T}{2^6 \pi^3 \mathcal{E}_N y_N} \frac{h_t^2 M \tilde{m}_1}{v^2} \int_{y_N}^{\infty} d\mathcal{E}_l \int_0^{\mathcal{E}_l + \mathcal{E}_N} d\mathcal{E}_t \Lambda_s^{(N)} I_s^{(1)},\tag{A.38}$$

$$\begin{aligned}I_s^{(1)} &= \int_{\mathcal{E}_l - y_N}^{\mathcal{E}_l + y_N} d\tilde{q} \frac{(\mathcal{E}_N + \mathcal{E}_l)^2 - z^2 - \tilde{q}^2}{(\mathcal{E}_N + \mathcal{E}_l)^2 - \tilde{q}^2} \\ &= \frac{4y_N (\mathcal{E}_l + \mathcal{E}_N) + z^2 \log \left[ \frac{(\mathcal{E}_N - y_N)(2\mathcal{E}_l + \mathcal{E}_N - y_N)}{(\mathcal{E}_N + y_N)(2\mathcal{E}_l + \mathcal{E}_N + y_N)} \right]}{2(\mathcal{E}_l + \mathcal{E}_N)}.\end{aligned}\tag{A.39}$$

- The second integral comes from evaluation of  $\Omega_{1b}$ :

$$C_{S,s}^{(2)} = \frac{3T}{2^6 \pi^3 \mathcal{E}_N y_N} \frac{h_t^2 M \tilde{m}_1}{v^2} \int_0^{y_N} d\mathcal{E}_l \int_0^{\mathcal{E}_l + \mathcal{E}_N} d\mathcal{E}_t \Lambda_s^{(N)} I_s^{(2)}, \quad (\text{A.40})$$

$$\begin{aligned} I_s^{(2)} &= \int_{y_N - \mathcal{E}_l}^{\mathcal{E}_l + y_N} d\tilde{q} \frac{(\mathcal{E}_N + \mathcal{E}_l)^2 - z^2 - \tilde{q}^2}{(\mathcal{E}_N + \mathcal{E}_l)^2 - \tilde{q}^2} \\ &= \frac{4 \mathcal{E}_l (\mathcal{E}_l + \mathcal{E}_N) + z^2 \log \left[ \frac{\mathcal{E}_N^2 - y_N^2}{(2\mathcal{E}_l + \mathcal{E}_N)^2 - y_N^2} \right]}{2 (\mathcal{E}_l + \mathcal{E}_N)}. \end{aligned} \quad (\text{A.41})$$

- The third integral comes from the  $\Omega_{2a,i}$  term:

$$C_{S,s}^{(3)} = \frac{3T}{2^6 \pi^3 \mathcal{E}_N y_N} \frac{h_t^2 M \tilde{m}_1}{v^2} \int_{y_N}^{\infty} d\mathcal{E}_l \int_0^{\frac{1}{2}(\mathcal{E}_N + y_N)} d\mathcal{E}_t \Lambda_s^{(N)} I_s^{(3)}, \quad (\text{A.42})$$

$$\begin{aligned} I_s^{(3)} &= - \int_{\mathcal{E}_l - y_N}^{\mathcal{E}_l + \mathcal{E}_N - 2\mathcal{E}_t} d\tilde{q} \frac{(\mathcal{E}_N + \mathcal{E}_l)^2 - z^2 - \tilde{q}^2}{(\mathcal{E}_N + \mathcal{E}_l)^2 - \tilde{q}^2} \\ &= - \frac{2 (\mathcal{E}_l + \mathcal{E}_N) (\mathcal{E}_N - 2\mathcal{E}_t + y_N) + z^2 \log \left[ \frac{\mathcal{E}_t (2\mathcal{E}_l + \mathcal{E}_N - y_N)}{(\mathcal{E}_l + \mathcal{E}_N - \mathcal{E}_t) (\mathcal{E}_N + y_N)} \right]}{2 (\mathcal{E}_l + \mathcal{E}_N)}. \end{aligned} \quad (\text{A.43})$$

- Integral four originates from the  $\Omega_{2a,ii}$  term:

$$C_{S,s}^{(4)} = \frac{3T}{2^6 \pi^3 \mathcal{E}_N y_N} \frac{h_t^2 M \tilde{m}_1}{v^2} \int_{y_N}^{\infty} d\mathcal{E}_l \int_{\frac{1}{2}(2\mathcal{E}_l + \mathcal{E}_N - y_N)}^{\mathcal{E}_l + \mathcal{E}_N} d\mathcal{E}_t \Lambda_s^{(N)} I_s^{(4)}, \quad (\text{A.44})$$

$$\begin{aligned} I_s^{(4)} &= - \int_{\mathcal{E}_l - y_N}^{2\mathcal{E}_t - \mathcal{E}_l - \mathcal{E}_N} d\tilde{q} \frac{(\mathcal{E}_N + \mathcal{E}_l)^2 - z^2 - \tilde{q}^2}{(\mathcal{E}_N + \mathcal{E}_l)^2 - \tilde{q}^2} \\ &= \frac{2 (\mathcal{E}_l + \mathcal{E}_N) (2\mathcal{E}_t + \mathcal{E}_N - 2\mathcal{E}_t - y_N) - z^2 \log \left[ \frac{(\mathcal{E}_l + \mathcal{E}_N - \mathcal{E}_t) (2\mathcal{E}_l + \mathcal{E}_N - y_N)}{\mathcal{E}_t (\mathcal{E}_N + y_N)} \right]}{2 (\mathcal{E}_l + \mathcal{E}_N)}. \end{aligned} \quad (\text{A.45})$$

- Integral five relates to  $\Omega_{2b,i}$ :

$$C_{S,s}^{(5)} = \frac{3T}{2^6 \pi^3 \mathcal{E}_N y_N} \frac{h_t^2 M \tilde{m}_1}{v^2} \int_0^{y_N} d\mathcal{E}_l \int_0^{\frac{1}{2}(2\mathcal{E}_l + \mathcal{E}_N - y_N)} d\mathcal{E}_t \Lambda_s^{(N)} I_s^{(5)}, \quad (\text{A.46})$$

$$\begin{aligned} I_s^{(5)} &= - \int_{y_N - \mathcal{E}_l}^{\mathcal{E}_l + \mathcal{E}_N - 2\mathcal{E}_t} d\tilde{q} \frac{(\mathcal{E}_N + \mathcal{E}_l)^2 - z^2 - \tilde{q}^2}{(\mathcal{E}_N + \mathcal{E}_l)^2 - \tilde{q}^2} \\ &= - \frac{2 (\mathcal{E}_l + \mathcal{E}_N) (2\mathcal{E}_t + \mathcal{E}_N - 2\mathcal{E}_t - y_N) - z^2 \log \left[ \frac{(\mathcal{E}_l + \mathcal{E}_N - \mathcal{E}_t) (2\mathcal{E}_l + \mathcal{E}_N - y_N)}{\mathcal{E}_t (\mathcal{E}_N + y_N)} \right]}{2 (\mathcal{E}_l + \mathcal{E}_N)}. \end{aligned} \quad (\text{A.47})$$

- Finally, the sixth integral derives from  $\Omega_{2b,ii}$ :

$$C_{S,s}^{(6)} = \frac{3T}{2^6 \pi^3 \mathcal{E}_N y_N} \frac{h_t^2 M \tilde{m}_1}{v^2} \int_0^{y_N} d\mathcal{E}_l \int_{\frac{1}{2}(\mathcal{E}_N + y_N)}^{\mathcal{E}_l + \mathcal{E}_N} d\mathcal{E}_t \Lambda_s^{(N)} I_s^{(6)}, \quad (\text{A.48})$$

$$\begin{aligned} I_s^{(6)} &= - \int_{y_N - \mathcal{E}_l}^{2\mathcal{E}_t - \mathcal{E}_l - \mathcal{E}_N} d\tilde{q} \frac{(\mathcal{E}_N + \mathcal{E}_l)^2 - z^2 - \tilde{q}^2}{(\mathcal{E}_N + \mathcal{E}_l)^2 - \tilde{q}^2} \\ &= \frac{2(\mathcal{E}_l + \mathcal{E}_N)(\mathcal{E}_N - 2\mathcal{E}_t + y_N) - z^2 \log \left[ \frac{(\mathcal{E}_l + \mathcal{E}_N - \mathcal{E}_t)(\mathcal{E}_N + y_N)}{\mathcal{E}_t(2\mathcal{E}_l + \mathcal{E}_N - y_N)} \right]}{2(\mathcal{E}_l + \mathcal{E}_N)}. \end{aligned} \quad (\text{A.49})$$

### A.1.2 Lepton asymmetry

The  $s$ -channel collision term in Eq. (4.22) for tracking the lepton asymmetry is

$$C_{S,s}[f_{l-\bar{l}}] = \frac{1}{2E_l} \int \prod_{i=N,q,t} \frac{dp_i^3}{(2\pi)^3 2E_i} (2\pi)^4 \delta^4(p_l + p_N - p_q - p_t) |\mathcal{M}_s|^2 \Lambda_s^{(l-\bar{l})} (f_{l-\bar{l}}, f_N, f_t, t_q), \quad (\text{A.50})$$

with phase space factor

$$\Lambda_s^{(l-\bar{l})} (f_{l-\bar{l}}, f_N, f_t, t_q) = f_{l-\bar{l}} (f_N (f_t + f_q - 1) - f_t f_q), \quad (\text{A.51})$$

and matrix element  $\mathcal{M}_s$  given by Eq. (A.11).

Again we choose an explicit coordinate system and use rotational invariance

$$\begin{aligned} \mathbf{q} &= |\mathbf{q}| (0, 0, 1), \\ \mathbf{p}_l &= E_l (0, \sin \eta, \cos \eta), \\ \mathbf{p}_t &= E_t (\cos \phi \sin \vartheta, \sin \phi \sin \vartheta, \cos \vartheta). \end{aligned} \quad (\text{A.52})$$

Following the same procedure as in section A.1.1, we reduce the collision integral (A.50) to

$$\begin{aligned} C_{S,s}[f_{l-\bar{l}}] &= \frac{1}{2^7 \pi^3 E_l^2} \int d \cos \vartheta d \cos \eta dE_t dE_N dq |\mathcal{M}_s|^2 \\ &\times \delta \left( \cos \eta - \frac{E_l^2 - E_N^2 + M + |\mathbf{q}|^2}{2|\mathbf{q}|E_l} \right) \delta \left( \cos \vartheta - \frac{E_t^2 - (E_l + E_N - E_t)^2 + |\mathbf{q}|^2}{2|\mathbf{q}|E_t} \right) \\ &\times \Lambda_s^{(l-\bar{l})} (f_{l-\bar{l}}, f_N, f_t, t_q) \Theta(E_N) \Theta(E_t) \Theta(E_l + E_N - E_t), \end{aligned} \quad (\text{A.53})$$

with phase space element

$$\Lambda_s^{(l-\bar{l})} (f_{l-\bar{l}}, f_N, f_t, t_q) = -f_{l-\bar{l}} \frac{e^{\mathcal{E}_t} (1 + (e^{\mathcal{E}_l + \mathcal{E}_N} - 1) f_N)}{(1 + e^{\mathcal{E}_t}) (e^{\mathcal{E}_l + \mathcal{E}_N} + e^{\mathcal{E}_t})}, \quad (\text{A.54})$$

using as usual energy conservation, and Fermi–Dirac statistics for the leptons and quarks.

In analogy to section A.1.1, we further reduce the collision integral (A.53) to a sum of six integrals with distinct integration ranges,

$$C_{S,s}[f_{l-\bar{l}}] = C_{S,s}^{(1)} + C_{S,s}^{(2)} + C_{S,s}^{(3)} + C_{S,s}^{(4)} + C_{S,s}^{(5)} + C_{S,s}^{(6)}, \quad (\text{A.55})$$

to be integrated numerically over two remaining degrees of freedom. These integrals are:

- First integral

$$C_{S,s}^{(1)} = \frac{3T}{2^6 \pi^3 \mathcal{E}_l^2} \frac{h_t^2 M \tilde{m}_1}{v^2} \int_z^{\sqrt{\mathcal{E}_l^2 + z^2}} d\mathcal{E}_N \int_0^{\mathcal{E}_l + \mathcal{E}_N} d\mathcal{E}_t \Lambda_s^{(l-\bar{l})} I_s^{(1)}, \quad (\text{A.56})$$

where  $I_s^{(1)}$  is given by Eq. (A.39).

- Second integral with  $I_s^{(2)}$  given by Eq. (A.41):

$$C_{S,s}^{(2)} = \frac{3T}{2^6 \pi^3 \mathcal{E}_l^2} \frac{h_t^2 M \tilde{m}_1}{v^2} \int_{\sqrt{\mathcal{E}_l^2 + z^2}}^{\infty} d\mathcal{E}_N \int_0^{\mathcal{E}_l + \mathcal{E}_N} d\mathcal{E}_t \Lambda_s^{(l-\bar{l})} I_s^{(2)}. \quad (\text{A.57})$$

- Third integral ( $I_s^{(3)}$  given by Eq. (A.43)):

$$C_{S,s}^{(3)} = \frac{3T}{2^6 \pi^3 \mathcal{E}_l^2} \frac{h_t^2 M \tilde{m}_1}{v^2} \int_z^{\sqrt{\mathcal{E}_l^2 + z^2}} d\mathcal{E}_N \int_0^{\frac{1}{2}(\mathcal{E}_N + y_N)} d\mathcal{E}_t \Lambda_s^{(l-\bar{l})} I_s^{(3)}. \quad (\text{A.58})$$

- Fourth integral ( $I_s^{(4)}$  given by Eq. (A.45)):

$$C_{S,s}^{(4)} = \frac{3T}{2^6 \pi^3 \mathcal{E}_l^2} \frac{h_t^2 M \tilde{m}_1}{v^2} \int_z^{\sqrt{\mathcal{E}_l^2 + z^2}} d\mathcal{E}_N \int_{\frac{1}{2}(2\mathcal{E}_l + \mathcal{E}_N - y_N)}^{\mathcal{E}_l + \mathcal{E}_N} d\mathcal{E}_t \Lambda_s^{(l-\bar{l})} I_s^{(4)}. \quad (\text{A.59})$$

- Fifth integral ( $I_s^{(5)}$  given by Eq. (A.47)):

$$C_{S,s}^{(5)} = \frac{3T}{2^6 \pi^3 \mathcal{E}_l^2} \frac{h_t^2 M \tilde{m}_1}{v^2} \int_{\sqrt{\mathcal{E}_l^2 + z^2}}^{\infty} d\mathcal{E}_N \int_0^{\frac{1}{2}(2\mathcal{E}_l + \mathcal{E}_N - y_N)} d\mathcal{E}_t \Lambda_s^{(l-\bar{l})} I_s^{(5)}. \quad (\text{A.60})$$

- sixth integral ( $I_s^{(6)}$  given by Eq. (A.49)):

$$C_{S,s}^{(6)} = \frac{3T}{2^6 \pi^3 \mathcal{E}_l^2} \frac{h_t^2 M \tilde{m}_1}{v^2} \int_{\sqrt{\mathcal{E}_l^2 + z^2}}^{\infty} d\mathcal{E}_N \int_{\frac{1}{2}(\mathcal{E}_N + y_N)}^{\mathcal{E}_l + \mathcal{E}_N} d\mathcal{E}_t \Lambda_s^{(l-\bar{l})} I_s^{(6)}. \quad (\text{A.61})$$

## A.2 $t$ -channel

### A.2.1 Right-handed neutrino

The collision integral for the  $t$ -channel process appearing in Eq. (4.20) is given by

$$C_{S,t}[f_N] = \frac{1}{2E_N} \int \prod_{i=l,q,t} \frac{dp_i^3}{(2\pi)^3 2E_i} (2\pi)^4 \delta^4(p_N + p_q - p_t - p_l) |\mathcal{M}_t|^2 \Lambda_t^{(N)}(f_N, f_q, f_l, f_t), \quad (\text{A.62})$$

with phase space factor

$$\Lambda_t^{(N)}(f_N, f_q, f_l, f_t) = [(1 - f_N)(1 - f_q) f_t f_l - f_N f_q (1 - f_t)(1 - f_l)], \quad (\text{A.63})$$

and

$$|\mathcal{M}_t|^2 = 24 h_t^2 \frac{M \tilde{m}_1}{v^2} \frac{p_N p_l p_q p_t}{t^2} \quad (\text{A.64})$$



is the matrix element.

The reduction of the collision integral proceeds in the same way as for the analogous  $s$ -channel collision integral in section A.1. We use the momentum

$$\mathbf{k} \equiv \mathbf{p}_l - \mathbf{p}_N = \mathbf{p}_q - \mathbf{p}_t, \quad (\text{A.65})$$

and coordinates

$$\begin{aligned} \mathbf{k} &= |\mathbf{k}| (0, 0, 1), \\ \mathbf{p}_q &= E_q (0, \sin \eta, \cos \eta), \\ \mathbf{p}_N &= |\mathbf{p}_N| (\cos \phi \sin \vartheta, \sin \phi \sin \vartheta, \cos \vartheta). \end{aligned} \quad (\text{A.66})$$

The matrix element in these coordinates reads

$$|\mathcal{M}_t|^2 = 6 h_t^2 \frac{M \tilde{m}_1}{v^2} \frac{(E_N - E_l)^2 - M^2 - |\mathbf{k}|^2}{(E_N - E_l)^2 - |\mathbf{k}|^2}. \quad (\text{A.67})$$

Averaging over the incoming RHN direction and integrating over all azimuthal angles leads to the following 5-dimensional integral:

$$\begin{aligned} C_{S,t}[f_N] &= \frac{1}{2^7 \pi^3 E_N p_N} \int d \cos \vartheta d \cos \eta d E_q d E_l d |\mathbf{k}| |\mathcal{M}_t|^2 \\ &\times \delta \left( \cos \eta + \frac{(E_N + E_q - E_l)^2 - E_q^2 - |\mathbf{k}|^2}{2 |\mathbf{k}| E_q} \right) \delta \left( \cos \vartheta - \frac{E_l^2 - E_N^2 + M - |\mathbf{k}|^2}{2 |\mathbf{k}| |\mathbf{p}_N|} \right) \\ &\times \Lambda_t^{(N)}(f_N, f_q, f_l, f_t) \Theta(E_q) \Theta(E_l) \Theta(E_N + E_q - E_l), \end{aligned} \quad (\text{A.68})$$

with

$$\Lambda_t^{(N)}(f_N, f_q, f_l, f_t) = - \frac{e^{\mathcal{E}_l + \mathcal{E}_q} (-1 + f_N + e^{\mathcal{E}_N} f_N)}{(1 + e^{\mathcal{E}_l}) (1 + e^{\mathcal{E}_q}) (e^{\mathcal{E}_l} + e^{\mathcal{E}_l + \mathcal{E}_q})}, \quad (\text{A.69})$$

assuming thermal equilibrium for the standard model particles.

The integrals over  $\cos \eta$  and  $\cos \vartheta$  in Eq. (A.68) can be readily performed in the same manner as before, and, in the process, integration limits are derived for the integral over  $k = |\mathbf{k}|$ . As it turns out, there are two possible lower limits for the  $k$ -integration:  $k_{\min,1} = E_N - E_l$  and  $k_{\min,2} = E_l - p_N$ . Here, a comment on the infrared cut-off is in order. In the integrated picture, a divergence occurs in the integral over  $t$  at  $t = 0$ , whose regulation requires the introduction of a Higgs mass in the propagator, i.e.,  $|\mathcal{M}_t|^2 \propto 1/t \rightarrow |\mathcal{M}_t|^2 \propto 1/(t - m_\Phi^2)$ . In the full treatment, the matrix element has the form  $|\mathcal{M}_t|^2 \propto 1/((E_N - E_l)^2 - k^2)$ , so that the equivalent divergence occurs in the integration over  $k$  at  $k = E_N - E_l$ , i.e., at  $k = k_{\min,1}$ . This divergence can be avoided simply by modifying by hand the integration limit  $\int_{k_{\min,1}} \rightarrow \int_{k_{\min,1} + m_\Phi}$ . There are no changes for those integrals with  $k_{\min} = k_{\min,2}$ .

It is also possible to regulate the divergence by introducing a Higgs mass in the propagator, such as in the integrated picture. This modifies the integration over  $k$  not only for  $E_N > E_l$  (i.e.,  $k_{\min} = k_{\min,1}$ ), but also for  $E_l > p_N$  (i.e.,  $k_{\min} = k_{\min,2}$ ). In physical terms this procedure corresponds to giving the Higgs particle a mass whose magnitude can vary from zero up to possible thermal contributions, i.e.,  $0 \leq m_\Phi/M \lesssim 0.4 T/M$ , where  $m_\Phi(T) \sim 0.4 T$  is the thermal Higgs mass [6]. In the temperature regime relevant to leptogenesis, electroweak symmetry is unbroken and therefore leptons are massless.

Since we have so far not included thermal corrections in the present work, for consistency we prefer not to use the thermal Higgs mass. Furthermore, in a full thermal treatment, RHN decay into a lepton and Higgs pairs become kinematically forbidden at high enough temperatures, and the decay of a Higgs particle into a neutrino and lepton pair becomes viable [6]. Thus, in addition to determining the value of the infrared cut-off there is also the question of its interpretation. In view of these issues, we choose to deal with the infrared divergence using the simpler method of cutting off the integration over  $k$  at  $k_{\min} = k_{\min,1} + m_\Phi$ , with  $a_h = m_\Phi/M = 10^{-5}$ .

After integrating over  $\cos \eta$  and  $\cos \vartheta$ , the original integral (A.68) is now split into four parts

$$C_{S,t}[f_N] = C_{S,t}^{(1)} + C_{S,t}^{(2)} + C_{S,t}^{(3)} + C_{S,t}^{(4)}, \quad (\text{A.70})$$

where the constituent integrals are as follows:

- First integral (with  $\tilde{k} \equiv k/T$ ):

$$C_{S,t}^{(1)} = \frac{3T}{2^6 \pi^3 \mathcal{E}_N y_N} \frac{h_t^2 M \tilde{m}_1}{v^2} \int_{\frac{1}{2}(\mathcal{E}_N - y_N + a_h z)}^{\frac{1}{2}(\mathcal{E}_N + y_N)} d\mathcal{E}_l \int_{\frac{1}{2} a_h z}^{\frac{1}{2}(2\mathcal{E}_l - \mathcal{E}_N + y_N)} d\mathcal{E}_q \Lambda_t^{(N)} I_t^{(1)}, \quad (\text{A.71})$$

$$I_t^{(1)} = \int_{\mathcal{E}_N - \mathcal{E}_l + a_h z}^{2\mathcal{E}_q + \mathcal{E}_N - \mathcal{E}_l} d\tilde{k} \frac{(\mathcal{E}_N - \mathcal{E}_l)^2 - z^2 - \tilde{k}^2}{(\mathcal{E}_N - \mathcal{E}_l)^2 - \tilde{k}^2}$$

$$= \frac{2(\mathcal{E}_N - \mathcal{E}_l)(2\mathcal{E}_q - a_h z) - z^2 \log \left[ \frac{(\mathcal{E}_N + \mathcal{E}_q - \mathcal{E}_l) a_h z}{\mathcal{E}_q (2(\mathcal{E}_N - \mathcal{E}_l) + a_h z)} \right]}{2(\mathcal{E}_N - \mathcal{E}_l)}.$$

- Second integral:

$$C_{S,t}^{(2)} = \frac{3T}{2^6 \pi^3 \mathcal{E}_N y_N} \frac{h_t^2 M \tilde{m}_1}{v^2} \int_{\frac{1}{2}(\mathcal{E}_N - y_N + a_h z)}^{\frac{1}{2}(\mathcal{E}_N + y_N)} d\mathcal{E}_l \int_{\frac{1}{2}(2\mathcal{E}_l - \mathcal{E}_N + y_N)}^{\infty} d\mathcal{E}_q \Lambda_t^{(N)} I_t^{(2)}, \quad (\text{A.72})$$

$$I_t^{(2)} = \int_{\mathcal{E}_N - \mathcal{E}_l + a_h z}^{\mathcal{E}_l + y_N} d\tilde{k} \frac{(\mathcal{E}_N - \mathcal{E}_l)^2 - z^2 - \tilde{k}^2}{(\mathcal{E}_N - \mathcal{E}_l)^2 - \tilde{k}^2}$$

$$= \frac{2(\mathcal{E}_N - \mathcal{E}_l)(2\mathcal{E}_l - \mathcal{E}_N + y_N - a_h z) - z^2 \left( \log \left[ \frac{-a_h z (\mathcal{E}_N + y_N)}{(\mathcal{E}_N - 2\mathcal{E}_l - y_N)(2(\mathcal{E}_N - \mathcal{E}_l) + a_h z)} \right] \right)}{2(\mathcal{E}_N - \mathcal{E}_l)}.$$

- Third integral:

$$C_{S,t}^{(3)} = \frac{3T}{2^6 \pi^3 \mathcal{E}_N y_N} \frac{h_t^2 M \tilde{m}_1}{v^2} \int_{\frac{1}{2}(\mathcal{E}_N + y_N)}^{\infty} d\mathcal{E}_l \int_{\frac{1}{2}(2\mathcal{E}_l - \mathcal{E}_N - y_N)}^{\frac{1}{2}(2\mathcal{E}_l - \mathcal{E}_N + y_N)} d\mathcal{E}_q \Lambda_t^{(N)} I_t^{(3)}, \quad (\text{A.73})$$

$$I_t^{(3)} = \int_{\mathcal{E}_l - y_N}^{2\mathcal{E}_q + \mathcal{E}_N - \mathcal{E}_l} d\tilde{k} \frac{(\mathcal{E}_N - \mathcal{E}_l)^2 - z^2 - \tilde{k}^2}{(\mathcal{E}_N - \mathcal{E}_l)^2 - \tilde{k}^2}$$

$$= \frac{2(\mathcal{E}_N - \mathcal{E}_l)(\mathcal{E}_N + y_N + 2(\mathcal{E}_q - \mathcal{E}_l)) + z^2 \left( \log \left[ -\frac{-\mathcal{E}_q (\mathcal{E}_N - y_N)}{(\mathcal{E}_N + \mathcal{E}_q - \mathcal{E}_l)(\mathcal{E}_N - 2\mathcal{E}_l + y_N)} \right] \right)}{2(\mathcal{E}_N - \mathcal{E}_l)}.$$

- Fourth integral:

$$\begin{aligned}
C_{S,t}^{(4)} &= \frac{3T}{2^6 \pi^3 \mathcal{E}_N y_N} \frac{h_t^2 M \tilde{m}_1}{v^2} \int_{\frac{1}{2}(\mathcal{E}_N + y_N)}^{\infty} d\mathcal{E}_l \int_{\frac{1}{2}(\mathcal{E}_l - \mathcal{E}_N + y_N)}^{\infty} d\mathcal{E}_q \Lambda_t^{(N)} I_t^{(4)}, \quad (\text{A.74}) \\
I_t^{(4)} &= \int_{\mathcal{E}_l - y_N}^{\mathcal{E}_l + y_N} d\tilde{k} \frac{(\mathcal{E}_N - \mathcal{E}_l)^2 - z^2 - \tilde{k}^2}{(\mathcal{E}_N - \mathcal{E}_l)^2 - \tilde{k}^2} \\
&= \frac{4(\mathcal{E}_N - \mathcal{E}_l) y_N + z^2 \log \left[ \frac{(\mathcal{E}_N - y_N)(\mathcal{E}_N - y_N - 2\mathcal{E}_l)}{(\mathcal{E}_N + y_N)(\mathcal{E}_N + y_N - 2\mathcal{E}_l)} \right]}{2(\mathcal{E}_N - \mathcal{E}_l)}.
\end{aligned}$$

## A.2.2 Lepton asymmetry

The  $t$ -channel collision integral for the lepton asymmetry evolution is

$$C_{S,t}[f_{l-\bar{l}}] = \frac{1}{2E_l} \int \prod_{i=N,q,t} \frac{dp_i^3}{(2\pi)^3 2E_i} (2\pi)^4 \delta^4(p_l + p_q - p_N - p_t) |\mathcal{M}_t|^2 \Lambda_t^{(l-\bar{l})} (f_{l-\bar{l}}, f_t, f_N, f_q), \quad (\text{A.75})$$

with

$$\Lambda_t^{(l-\bar{l})} (f_{l-\bar{l}}, f_t, f_N, f_q) = f_{l-\bar{l}} (f_q (f_t + f_N - 1) - f_t f_N). \quad (\text{A.76})$$

The matrix element is the same as for the RHN given in Eq. (A.64), and we use the momentum

$$\mathbf{k} \equiv \mathbf{p}_N - \mathbf{p}_l = \mathbf{p}_q - \mathbf{p}_t, \quad (\text{A.77})$$

and coordinates

$$\begin{aligned}
\mathbf{k} &= |\mathbf{k}| (0, 0, 1), \quad (\text{A.78}) \\
\mathbf{p}_q &= E_q (0, \sin \eta, \cos \eta), \\
\mathbf{p}_l &= E_l (\cos \phi \sin \vartheta, \sin \phi \sin \vartheta, \cos \vartheta).
\end{aligned}$$

Following the method of the previous sections, we reduce the integral (A.75) to

$$\begin{aligned}
C_{S,t}[f_{l-\bar{l}}] &= \frac{1}{2^7 \pi^3 E_l^2} \int d\cos \vartheta d\cos \eta dE_q dE_N d|\mathbf{k}| |\mathcal{M}_t|^2 \\
&\times \delta \left( \cos \eta + \frac{(E_l + E_q - E_N)^2 - E_q^2 - |\mathbf{k}|^2}{2|\mathbf{k}| E_q} \right) \delta \left( \cos \vartheta - \frac{E_N^2 - E_l^2 - M^2 - |\mathbf{k}|^2}{2|\mathbf{k}| E_l} \right) \\
&\times \Lambda_t^{(l-\bar{l})} (f_{l-\bar{l}}, f_t, f_N, f_q) \Theta(E_q) \Theta(E_N) \Theta(E_l + E_q - E_N), \quad (\text{A.79})
\end{aligned}$$

with

$$\Lambda_t^{(l-\bar{l})} (f_{l-\bar{l}}, f_t, f_N, f_q) = f_{l-\bar{l}} \frac{e^{\mathcal{E}_q} (e^{\mathcal{E}_l} (-1 + f_N) - e^{\mathcal{E}_N} f_N)}{(1 + e^{\mathcal{E}_q}) (e^{\mathcal{E}_N} + e^{\mathcal{E}_q + \mathcal{E}_l})} \quad (\text{A.80})$$

as the phase space factor.

Integrating over  $\cos \eta$  and  $\cos \vartheta$ , we split up the integral (A.79) into four parts,

$$C_{S,t}[f_{l-\bar{l}}] = C_{S,t}^{(1)} + C_{S,t}^{(2)} + C_{S,t}^{(3)} + C_{S,t}^{(4)}, \quad (\text{A.81})$$

with:

- First integral:

$$C_{S,t}^{(1)} = \frac{3T}{2^6 \pi^3 \mathcal{E}_N y_N} \frac{h_t^2 M \tilde{m}_1}{v^2} \int_{\frac{(2\mathcal{E}_l - a_h z)^2 + z^2}{2(2\mathcal{E}_l - a_h z)}}^{\infty} d\mathcal{E}_N \int_{\mathcal{E}_N - \mathcal{E}_l + \frac{1}{2}a_h z}^{\frac{1}{2}(\mathcal{E}_N + y_N)} d\mathcal{E}_q \Lambda_t^{(l-\bar{l})} I_t^{(1)}, \quad (\text{A.82})$$

$$I_t^{(1)} = \int_{\mathcal{E}_N - \mathcal{E}_l + a_h z}^{2\mathcal{E}_q + \mathcal{E}_l - \mathcal{E}_N} d\tilde{k} \frac{(\mathcal{E}_N - \mathcal{E}_l)^2 - z^2 - \tilde{k}^2}{(\mathcal{E}_N - \mathcal{E}_l)^2 - \tilde{k}^2}$$

$$= - \frac{2(\mathcal{E}_N - \mathcal{E}_l)(2(\mathcal{E}_N - \mathcal{E}_q - \mathcal{E}_l) + a_h z) + z^2 \log \left[ \frac{\mathcal{E}_q a_h z}{(\mathcal{E}_q - \mathcal{E}_N + \mathcal{E}_l)(2(\mathcal{E}_N - \mathcal{E}_l) + a_h z)} \right]}{2(\mathcal{E}_N - \mathcal{E}_l)}.$$

- Second integral:

$$C_{S,t}^{(2)} = \frac{3T}{2^6 \pi^3 \mathcal{E}_N y_N} \frac{h_t^2 M \tilde{m}_1}{v^2} \int_{\frac{(2\mathcal{E}_l - a_h z)^2 + z^2}{2(2\mathcal{E}_l - a_h z)}}^{\infty} d\mathcal{E}_N \int_{\frac{1}{2}(\mathcal{E}_N + y_N)}^{\infty} d\mathcal{E}_q \Lambda_t^{(l-\bar{l})} I_t^{(2)}, \quad (\text{A.83})$$

$$I_t^{(2)} = \int_{\mathcal{E}_N - \mathcal{E}_l + a_h z}^{\mathcal{E}_l + y_N} d\tilde{k} \frac{(\mathcal{E}_N - \mathcal{E}_l)^2 - z^2 - \tilde{k}^2}{(\mathcal{E}_N - \mathcal{E}_l)^2 - \tilde{k}^2}$$

$$= \frac{2(\mathcal{E}_N - \mathcal{E}_l)(2\mathcal{E}_l - \mathcal{E}_N + y_N - a_h z) - z^2 \log \left[ \frac{(\mathcal{E}_N + y_N) a_h z}{(2\mathcal{E}_l - \mathcal{E}_N + y_N)(2(\mathcal{E}_N - \mathcal{E}_l) + a_h z)} \right]}{2(\mathcal{E}_N - \mathcal{E}_l)}.$$

- Third integral:

$$C_{S,t}^{(3)} = \frac{3T}{2^6 \pi^3 \mathcal{E}_N y_N} \frac{h_t^2 M \tilde{m}_1}{v^2} \int_z^{\frac{4\mathcal{E}_l^2 + z^2}{4\mathcal{E}_l}} d\mathcal{E}_N \int_{\frac{1}{2}(\mathcal{E}_N - y_N)}^{\frac{1}{2}(\mathcal{E}_N + y_N)} d\mathcal{E}_q \Lambda_t^{(l-\bar{l})} I_t^{(3)}, \quad (\text{A.84})$$

$$I_t^{(3)} = \int_{\mathcal{E}_l - y_N}^{2\mathcal{E}_q + \mathcal{E}_l - \mathcal{E}_N} d\tilde{k} \frac{(\mathcal{E}_N - \mathcal{E}_l)^2 - z^2 - \tilde{k}^2}{(\mathcal{E}_N - \mathcal{E}_l)^2 - \tilde{k}^2}$$

$$= \frac{2(\mathcal{E}_N - \mathcal{E}_l)(2\mathcal{E}_q - \mathcal{E}_N + y_N) + z^2 \log \left[ \frac{(\mathcal{E}_N - \mathcal{E}_q - \mathcal{E}_l)(\mathcal{E}_N - y_N)}{\mathcal{E}_q(\mathcal{E}_N - 2\mathcal{E}_l + y_N)} \right]}{2(\mathcal{E}_N - \mathcal{E}_l)}.$$

- Fourth integral:

$$C_{S,t}^{(4)} = \frac{3T}{2^6 \pi^3 \mathcal{E}_N y_N} \frac{h_t^2 M \tilde{m}_1}{v^2} \int_z^{\frac{4\mathcal{E}_l^2 + z^2}{4\mathcal{E}_l}} d\mathcal{E}_N \int_{\frac{1}{2}(\mathcal{E}_N + y_N)}^{\infty} d\mathcal{E}_q \Lambda_t^{(l-\bar{l})} I_t^{(4)}, \quad (\text{A.85})$$

$$I_t^{(4)} = \int_{\mathcal{E}_l - y_N}^{\mathcal{E}_l + y_N} d\tilde{k} \frac{(\mathcal{E}_N - \mathcal{E}_l)^2 - z^2 - \tilde{k}^2}{(\mathcal{E}_N - \mathcal{E}_l)^2 - \tilde{k}^2}$$

$$= \frac{4(\mathcal{E}_N - \mathcal{E}_l)y_N + z^2 \log \left[ \frac{(\mathcal{E}_N - 2\mathcal{E}_l - y_N)(\mathcal{E}_N - y_N)}{(\mathcal{E}_N - 2\mathcal{E}_l + y_N)(\mathcal{E}_N + y_N)} \right]}{2(\mathcal{E}_N - \mathcal{E}_l)}.$$

## B. Evolution of the top Yukawa coupling

To determine the gauge and Yukawa couplings at some energy scale  $\mu \equiv \log(T/m_Z)$ , we use the renormalisation group equation,

$$\frac{dg_i^2}{d\mu} = \frac{c_1}{8\pi^2} g_i^4. \quad (\text{B.1})$$

where  $i$  denotes the corresponding gauge group of the standard model. The constants for the gauge couplings are

$$(c_1, c_2, c_3) = \left( \frac{41}{10} \cdot \frac{5}{3}, \frac{16}{9}, -7 \right). \quad (\text{B.2})$$

At one loop the solution of (B.1) for the gauge couplings yields

$$g_i = \sqrt{\frac{g_i^2(\mu=0)}{1 - \frac{g_i^2(\mu=0)}{8\pi^2} \mu}}. \quad (\text{B.3})$$

Neglecting contributions from the bottom and charm Yukawa couplings, the renormalisation group equation for the top Yukawa coupling at one loop is given by [34]

$$\frac{h_t^2}{d\mu} = \frac{c_t}{8\pi^2} h_t^2 \left( h_t^2 - \frac{17}{54} \cdot \frac{5}{3} g_1^2 - \frac{1}{2} g_2^2 - \frac{16}{9} g_3^2 \right). \quad (\text{B.4})$$

A detailed study of the evolution of quantities relevant for leptogenesis can be found in [35].

## References

- [1] M. Fukugita and T. Yanagida, *Baryogenesis without grand unification*, *Phys. Lett.* **B174** (1986) 45.
- [2] P. Minkowski,  *$\mu \rightarrow e$  gamma at a rate of one out of 1-billion muon decays?*, *Phys. Lett.* **B67** (1977) 421.
- [3] F. R. Klinkhamer and N. S. Manton, *A saddle point solution in the weinberg-salam theory*, *Phys. Rev.* **D30** (1984) 2212.
- [4] M. Plümacher, *Baryon asymmetry, neutrino mixing and supersymmetric SO(10) unification*, *Nucl. Phys.* **B530** (1998) 207–246, [hep-ph/9704231].
- [5] L. Covi, N. Rius, E. Roulet, and F. Vissani, *Finite temperature effects on cp violating asymmetries*, *Phys. Rev.* **D57** (1998) 93–99, [hep-ph/9704366].
- [6] G. F. Giudice, A. Notari, M. Raidal, A. Riotto, and A. Strumia, *Towards a complete theory of thermal leptogenesis in the sm and mssm*, *Nucl. Phys.* **B685** (2004) 89–149, [hep-ph/0310123].
- [7] W. Buchmüller, P. Di Bari, and M. Plümacher, *Leptogenesis for pedestrians*, *Ann. Phys.* **315** (2005) 305–351, [hep-ph/0401240].
- [8] A. Abada, S. Davidson, F.-X. Josse-Michaux, M. Losada, and A. Riotto, *Flavour Issues in Leptogenesis*, *JCAP* **0604** (2006) 004, [hep-ph/0601083].
- [9] A. Abada *et. al.*, *Flavour matters in leptogenesis*, *JHEP* **09** (2006) 010, [hep-ph/0605281].
- [10] E. Nardi, Y. Nir, E. Roulet, and J. Racker, *The importance of flavor in leptogenesis*, *JHEP* **01** (2006) 164, [hep-ph/0601084].
- [11] S. Blanchet and P. Di Bari, *Flavor effects on leptogenesis predictions*, *JCAP* **0703** (2007) 018, [hep-ph/0607330].
- [12] A. Anisimov, S. Blanchet, and P. Di Bari, *Viability of Dirac phase leptogenesis*, *JCAP* **0804** (2008) 033, [arXiv:0707.3024].

- [13] S. Blanchet, P. Di Bari, and G. G. Raffelt, *Quantum Zeno effect and the impact of flavor in leptogenesis*, *JCAP* **0703** (2007) 012, [hep-ph/0611337].
- [14] M. Lindner and M. M. Müller, *Comparison of Boltzmann equations with quantum dynamics for scalar fields*, *Phys. Rev.* **D73** (2006) 125002, [hep-ph/0512147].
- [15] M. Lindner and M. M. Müller, *Comparison of Boltzmann Kinetics with Quantum Dynamics for a Chiral Yukawa Model Far From Equilibrium*, *Phys. Rev.* **D77** (2008) 025027, [arXiv:0710.2917].
- [16] A. Basbøll and S. Hannestad, *Decay of heavy Majorana neutrinos using the full Boltzmann equation including its implications for leptogenesis*, *JCAP* **0701** (2007) 003, [hep-ph/0609025].
- [17] A. Sakharov *JETP Lett.* **5** (1967) 24.
- [18] E. W. Kolb and S. Wolfram, *Baryon Number Generation in the Early Universe*, *Nucl. Phys.* **B172** (1980) 224.
- [19] J. A. Harvey and M. S. Turner, *Cosmological baryon and lepton number in the presence of electroweak fermion number violation*, *Phys. Rev.* **D42** (1990) 3344–3349.
- [20] M. Plümacher, *Baryogenesis and lepton number violation*, *Z. Phys.* **C74** (1997) 549–559, [hep-ph/9604229].
- [21] J. Garayoa, S. Pastor, T. Pinto, N. Rius, and O. Vives, *On the full Boltzmann equations for Leptogenesis*, arXiv:0905.4834.
- [22] S. Blanchet and P. Di Bari, *Leptogenesis beyond the limit of hierarchical heavy neutrino masses*, *JCAP* **0606** (2006) 023, [hep-ph/0603107].
- [23] M. Kawasaki, G. Steigman, and H.-S. Kang, *Cosmological evolution of an early decaying particle*, *Nucl. Phys.* **B403** (1993) 671–706.
- [24] N. Kaiser, R. A. Malaney, and G. D. Starkman, *Neutrino lasing in the early universe*, *Phys. Rev. Lett.* **71** (1993) 1128–1131, [hep-ph/9302261].
- [25] W. Buchmüller, P. Di Bari, and M. Plümacher, *Cosmic microwave background, matter-antimatter asymmetry and neutrino masses*, *Nucl. Phys.* **B643** (2002) 367–390, [hep-ph/0205349].
- [26] F. Hahn-Woernle and M. Plümacher, *Effects of reheating on leptogenesis*, *Nucl. Phys.* **B806** (2009) 68–83, [arXiv:0801.3972].
- [27] A. Pilaftsis and T. E. J. Underwood, *Resonant leptogenesis*, *Nucl. Phys.* **B692** (2004) 303–345, [hep-ph/0309342].
- [28] A. Pilaftsis and T. E. J. Underwood, *Electroweak-scale resonant leptogenesis*, *Phys. Rev.* **D72** (2005) 113001, [hep-ph/0506107].
- [29] E. Nardi, J. Racker, and E. Roulet, *CP violation in scatterings, three body processes and the Boltzmann equations for leptogenesis*, *JHEP* **09** (2007) 090, [arXiv:0707.0378].
- [30] M. A. Luty, *Baryogenesis via leptogenesis*, *Phys. Rev.* **D45** (1992) 455–465.
- [31] M. Bolz, A. Brandenburg, and W. Buchmüller, *Thermal production of gravitinos*, *Nucl. Phys.* **B606** (2001) 518–544, [hep-ph/0012052].
- [32] J. Pradler, *Electroweak Contributions to Thermal Gravitino Production*, arXiv:0708.2786.
- [33] A. Hohenegger, *Solving the Homogeneous Boltzmann Equation with Arbitrary Scattering Kernel*, arXiv:0806.3098.

- [34] M. Lindner, *Implications of Triviality for the Standard Model*, *Zeit. Phys.* **C31** (1986) 295.
- [35] S. Antusch, J. Kersten, M. Lindner, M. Ratz, and M. A. Schmidt, *Running neutrino mass parameters in see-saw scenarios*, *JHEP* **03** (2005) 024, [[hep-ph/0501272](#)].